



DNA Damage Signaling Is Required for Replication of Human Bocavirus 1 DNA in Dividing HEK293 Cells

Xuefeng Deng,^a Peng Xu,^{a,b} Wei Zou,^a Weiran Shen,^a Jianxin Peng,^b Kaiyu Liu,^b John F. Engelhardt,^c Ziyang Yan,^c Jianming Qiu^a

Department of Microbiology, Molecular Genetics and Immunology, University of Kansas Medical Center, Kansas City, Kansas, USA^a; College of Life Sciences, Central China Normal University, Wuhan, China^b; Department of Anatomy and Cell Biology, University of Iowa, Iowa City, Iowa, USA^c

ABSTRACT Human bocavirus 1 (HBoV1), an emerging human-pathogenic respiratory virus, is a member of the genus *Bocaparvovirus* of the *Parvoviridae* family. In human airway epithelium air-liquid interface (HAE-ALI) cultures, HBoV1 infection initiates a DNA damage response (DDR), activating all three phosphatidylinositol 3-kinase-related kinases (PI3KKs): ATM, ATR, and DNA-PKcs. In this context, activation of PI3KKs is a requirement for amplification of the HBoV1 genome (X. Deng, Z. Yan, F. Cheng, J. F. Engelhardt, and J. Qiu, *PLoS Pathog*, 12:e1005399, 2016, <https://doi.org/10.1371/journal.ppat.1005399>), and HBoV1 replicates only in terminally differentiated, nondividing cells. This report builds on the previous discovery that the replication of HBoV1 DNA can also occur in dividing HEK293 cells, demonstrating that such replication is likewise dependent on a DDR. Transfection of HEK293 cells with the duplex DNA genome of HBoV1 induces hallmarks of DDR, including phosphorylation of H2AX and RPA32, as well as activation of all three PI3KKs. The large viral nonstructural protein NS1 is sufficient to induce the DDR and the activation of the three PI3KKs. Pharmacological inhibition or knockdown of any one of the PI3KKs significantly decreases both the replication of HBoV1 DNA and the downstream production of progeny virions. The DDR induced by the HBoV1 NS1 protein does not cause obvious damage to cellular DNA or arrest of the cell cycle. Notably, key DNA replication factors and major DNA repair DNA polymerases (polymerase η [Pol η] and polymerase κ [Pol κ]) are recruited to the viral DNA replication centers and facilitate HBoV1 DNA replication. Our study provides the first evidence of the DDR-dependent parvovirus DNA replication that occurs in dividing cells and is independent of cell cycle arrest.

IMPORTANCE The parvovirus human bocavirus 1 (HBoV1) is an emerging respiratory virus that causes lower respiratory tract infections in young children worldwide. HEK293 cells are the only dividing cells tested that fully support the replication of the duplex genome of this virus and allow the production of progeny virions. In this study, we demonstrate that HBoV1 induces a DDR that plays significant roles in the replication of the viral DNA and the production of progeny virions in HEK293 cells. We also show that both cellular DNA replication factors and DNA repair DNA polymerases colocalize within centers of viral DNA replication and that Pol η and Pol κ play an important role in HBoV1 DNA replication. Whereas the DDR that leads to the replication of the DNA of other parvoviruses is facilitated by the cell cycle, the DDR triggered by HBoV1 DNA replication or NS1 is not. HBoV1 is the first parvovirus whose NS1 has been shown to be able to activate all three PI3KKs (ATM, ATR, and DNA-PKcs).

KEYWORDS DNA damage, DNA replication, parvovirus

Received 12 September 2016 Accepted 5 October 2016

Accepted manuscript posted online 12 October 2016

Citation Deng X, Xu P, Zou W, Shen W, Peng J, Liu K, Engelhardt JF, Yan Z, Qiu J. 2017. DNA damage signaling is required for replication of human bocavirus 1 DNA in dividing HEK293 cells. *J Virol* 91:e01831-16. <https://doi.org/10.1128/JVI.01831-16>.

Editor Grant McFadden, University of Florida

Copyright © 2016 American Society for Microbiology. All Rights Reserved.

Address correspondence to Jianming Qiu, jqiu@kumc.edu.

Human bocavirus 1 (HBoV1) belongs to the species *Primate bocaparvovirus 1* of the genus *Bocaparvovirus* in the *Parvoviridae* family (1, 2). *Primate bocaparvovirus 1* also includes HBoV3 and gorilla bocavirus, whereas *Primate bocaparvovirus 2* includes strains HBoV2 and HBoV4. To date, the only bocaparvoviruses that have been isolated and cultured *in vitro* are HBoV1 (3), bovine parvovirus 1 (BPV1) (4), and minute virus of canines (MVC) (5). Other viruses were classified into this genus on the basis of the conservation of viral sequences encoding nonstructural (NS) and structural capsid (Cap) proteins (6–9). HBoV1 is an emerging human-pathogenic respiratory virus that causes lower respiratory tract infections in young children and is a health concern worldwide (10–21). *In vitro*, HBoV1 infects well-differentiated/polarized primary human airway epithelia (HAE) cultured at an air-liquid interface (ALI) (3, 22, 23). In addition, the duplex genome of HBoV1 replicates in human embryonic kidney 293 (HEK293) cells and produces progeny virions that are infectious for HAE-ALI cultures (22–24).

Five HBoV1 NS proteins have been identified through transfection of HEK293 cells with the HBoV1 duplex genome and HBoV1 infection of HAE-ALI cultures (25). These proteins are designated NS1, NS2, NS3, NS4, and NP1. NS1, -2, -3, and -4 are encoded on the left side of the HBoV1 genome and share a C terminus of 184 amino acid (aa) residues. Among them, NS1 is the largest one and is the only one essential for the replication of viral DNA (22). It contains a DNA origin-binding/endonuclease domain (OBD) at its N terminus, a helicase domain in the center, and a transactivation domain (TAD) at the C terminus (25). OBD has a canonical structure, as defined by the histidine-hydrophobic amino acid-histidine superfamily of nucleases; i.e., it combines two distinct DNA-binding sites (26). NS2 contains OBD and TAD, NS3 contains the helicase domain and TAD, and NS4 contains only TAD. An additional splice variant of NS1, NS1-70, has also been identified (27, 28). It contains only the OBD and helicase domain of NS1 (25). NS2 to NS4 are not required for the replication of the HBoV1 duplex genome in HEK293 cells, although NS2 is essential for virus replication in HAE-ALI cultures (25). The functions of NS1-70, NS3, and NS4 are currently unknown.

Bocaparvovirus genomes encode the nonstructural nuclear phosphoprotein NP1 (29) in the center of their genomes and in this respect are unique among parvoviruses. NP1 plays important roles not only in the replication of bocaparvovirus DNA (22, 30) but also in the processing of the viral pre-mRNA (31–33). It is essential to generate the mRNA that encodes viral capsid proteins VP1, VP2, and VP3 (33). HBoV1 NP1 colocalizes within the autonomous parvovirus-associated replication (APAR) bodies and complements the function of the minute virus of mice (MVM) NS2 protein in viral DNA replication during the early phase of infection (34).

The HBoV1 genome was efficiently amplified in mitotically quiescent airway epithelial cells of HAE-ALI cultures (35). As such, it represents a unique example of a genome of an autonomous parvovirus capable of *de novo* DNA synthesis in nondividing cells. HBoV1 infection of HAE-ALI cultures initiates a DNA damage response (DDR) that involves activation of all three phosphatidylinositol 3-kinase-related kinases (PI3KKs): ATM (ataxia telangiectasia mutated), ATR (ATM and RAD3 related), and DNA-PKcs (DNA-dependent protein kinase catalytic subunit). Activation of the three PI3KKs is required for amplification of the HBoV1 genome; more importantly, two members of the Y family of DNA polymerases, polymerase η (Pol η) and polymerase κ (Pol κ), are involved in this process (35). In contrast to HBoV1, all other known autonomous parvoviruses rely on the activity of the cellular DNA replication machinery during S phase for their replication (36–42). In dividing HEK293 cells, upon transfection of the HBoV1 duplex genome, the viral DNA replicates in these cells and progeny virions capable of efficiently infecting HAE-ALI cultures are generated (22). Additionally, a recombinant genome that carries a gene of interest flanked by extended left and right ends of the HBoV1 genome replicates in HEK293 cells, with the HBoV1 NS and Cap genes being provided in *trans*. These viral genomes can be packaged into HBoV1 capsids to produce a recombinant HBoV1 (rHBoV1) vector (43). Also, an HBoV1 capsid-pseudotyped recombinant adeno-associated virus type 2 (rAAV2/HBoV1) vector can be produced in HEK293 cells by transfecting an rAAV2 proviral plasmid together with

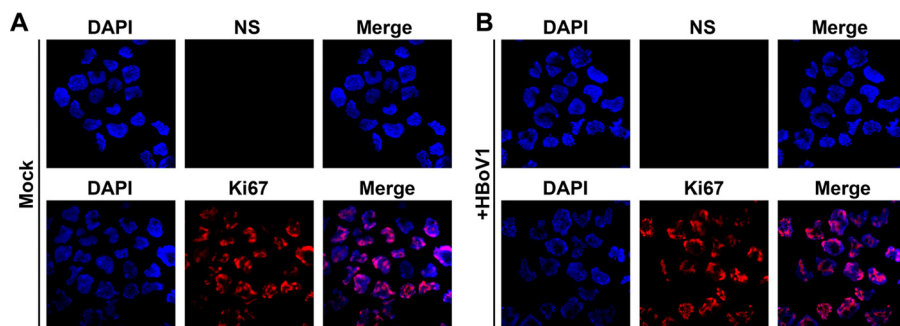


FIG 1 HBoV1 does not infect HEK293 cells. HEK293 cells were mock infected (A) or infected with HBoV1 at an MOI of ~ 400 vgc/cell (B). At 3 days postinfection, infected cells were analyzed by IF staining with anti-NS1C and anti-Ki67 antibodies. Nuclei were stained with DAPI, and confocal images were captured at a $\times 60$ magnification.

AAV2 Rep78-expressing and HBoV1 NS- and Cap-expressing helper plasmids, as well as an adenovirus-expressing helper plasmid (43). These recombinant HBoV1-based vectors demonstrate a remarkable tropism for human airway epithelia and a good potential as vehicles for the delivery of genes for gene therapy and vaccines targeting the human airways.

In this study, we sought to understand how the HBoV1 duplex genome replicates in HEK293 cells. We discovered the following: HBoV1 DNA induces a DDR in HEK293 cells, and this plays an important role in its replication; NS1 and its short isoform, NS1-70, are sufficient to induce the DDR; and HBoV1 DNA recruits most of the DNA replication factors as well as the DNA repair DNA polymerases into centers of viral DNA replication.

RESULTS

Transfection of HEK293 cells with the HBoV1 duplex genome induces a DDR.

HBoV1 does not infect proliferating airway epithelial cells (35). Similarly, proliferating HEK293 cells (as identified by immunoreactivity for Ki67) do not express NS proteins at detectable levels following infection with HBoV1 at multiplicities of infection (MOIs) as high as 400 viral genome copies (vgc) per cell (Fig. 1). However, HEK293 cells transfected with the HBoV1 duplex genome replicate viral DNA (22). On the basis of our previous observation that HAE-ALI cultures infected with HBoV1 mount a DNA damage response (DDR) (35), we hypothesized that replication of the HBoV1 duplex genome in HEK293 cells likewise induces this process. We addressed this through immunofluorescence (IF) and Western blot analyses, using hydroxyurea (HU) treatment as a positive control for the induction of DDR. The phosphorylation of mammalian replication protein A32 (RPA32) and the phosphorylation of histone variant H2AX (H2A histone family member X) are hallmarks of the DDR. In pIHBoV1-transfected cells, in which NS1 to NS4 were expressed, both RPA32 and H2AX were phosphorylated, as demonstrated by staining with antibodies against p-RPA32 (RPA32 phosphorylated on threonine 21) and γ H2AX (H2AX phosphorylated on serine 139) (Fig. 2A and B). Viral DNA replication centers stained positive with anti-NS1C and appeared at 12 h posttransfection; these centers colocalized well with foci that exhibited DDR (γ H2AX and p-RPA32). However, there was neither an obvious gradual enlargement of the replication centers nor an increase in DNA damage foci from 12 to 48 h posttransfection. Western blotting confirmed that HU treatment or transfection with pIHBoV1 induces the phosphorylation of RPA32 and H2AX in HEK293 cells (Fig. 2C). There was a gradual but less than 2-fold increase in the levels of expression of γ H2AX and p-RPA32 from 12 to 48 h posttransfection (Fig. 2D).

We next examined the activation status of the three PI3KKs which trigger the DDR (44, 45). As expected, ATM, ATR, and DNA-PKcs were all activated in pIHBoV1-transfected cells and colocalized with NS1 to NS4, as determined by staining with antibodies against the specifically phosphorylated site(s) of each kinase (Fig. 3A to D). Importantly, the DNA

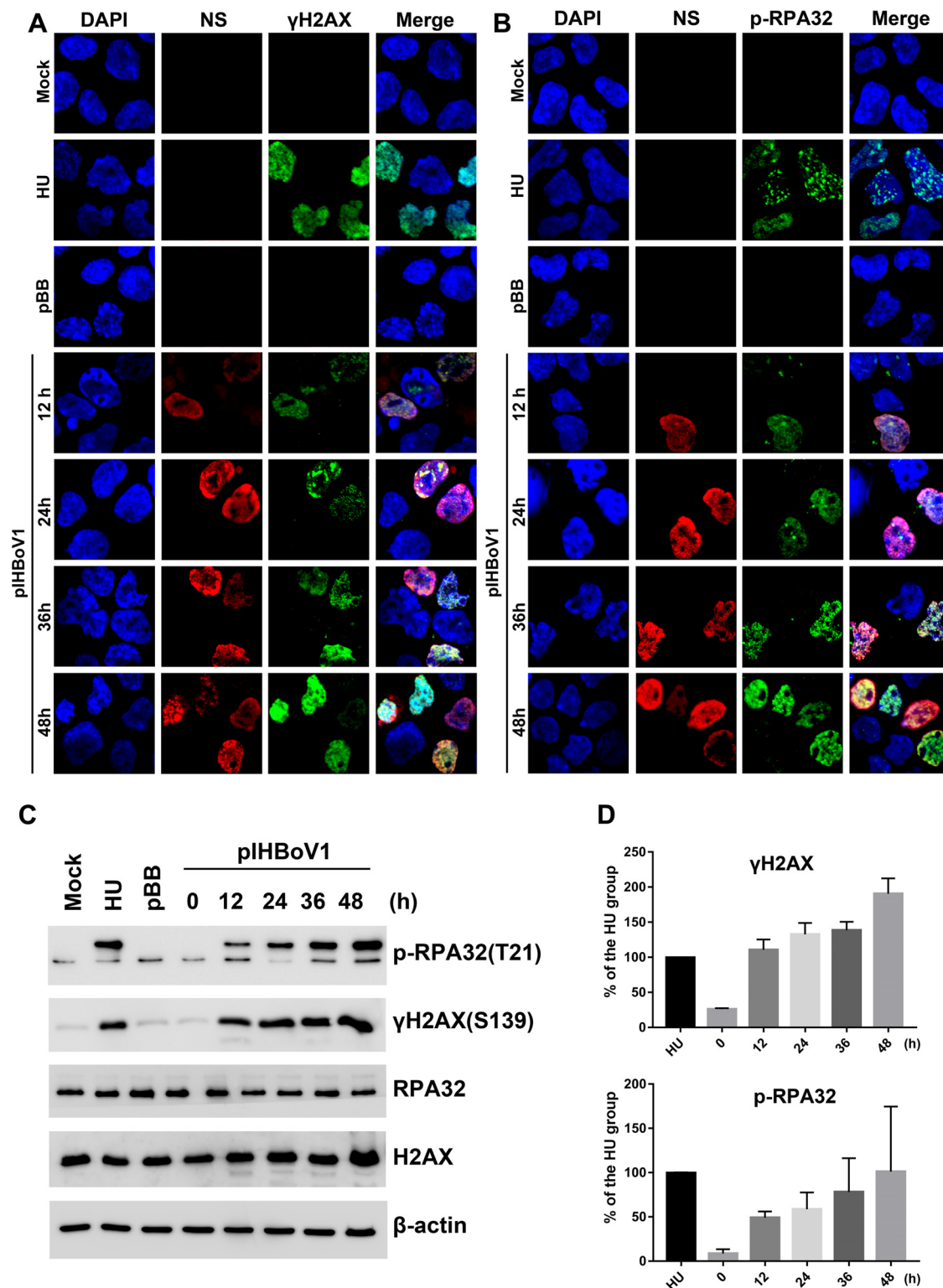


FIG 2 Transfection of pIHBoV1 induces a DDR in HEK293 cells. HEK293 cells were transfected with the HBov1 infectious clone pIHBoV1 or its backbone plasmid, pBB, and subjected to IF and Western blot analyses at the indicated times posttransfection. HU-treated cells were used as a DDR-positive control. (A and B) IF analysis. Cells were stained with anti-NS1C and anti- γ H2AX antibodies (A) and with anti-NS1C and anti-p-RPA32 antibodies (B). Nuclei were stained with DAPI. Confocal images were taken at a $\times 100$ magnification. (C and D) Western blot analysis. (C) The cells were analyzed by Western blotting using the antibodies anti- γ H2AX and anti-p-RPA32. β -Actin served as a loading control. (D) The levels of γ H2AX and p-RPA32 expression in each group were quantified, and the levels relative to those in HU-treated cells were calculated and plotted. Averages and standard deviations obtained from three independent experiments are shown.

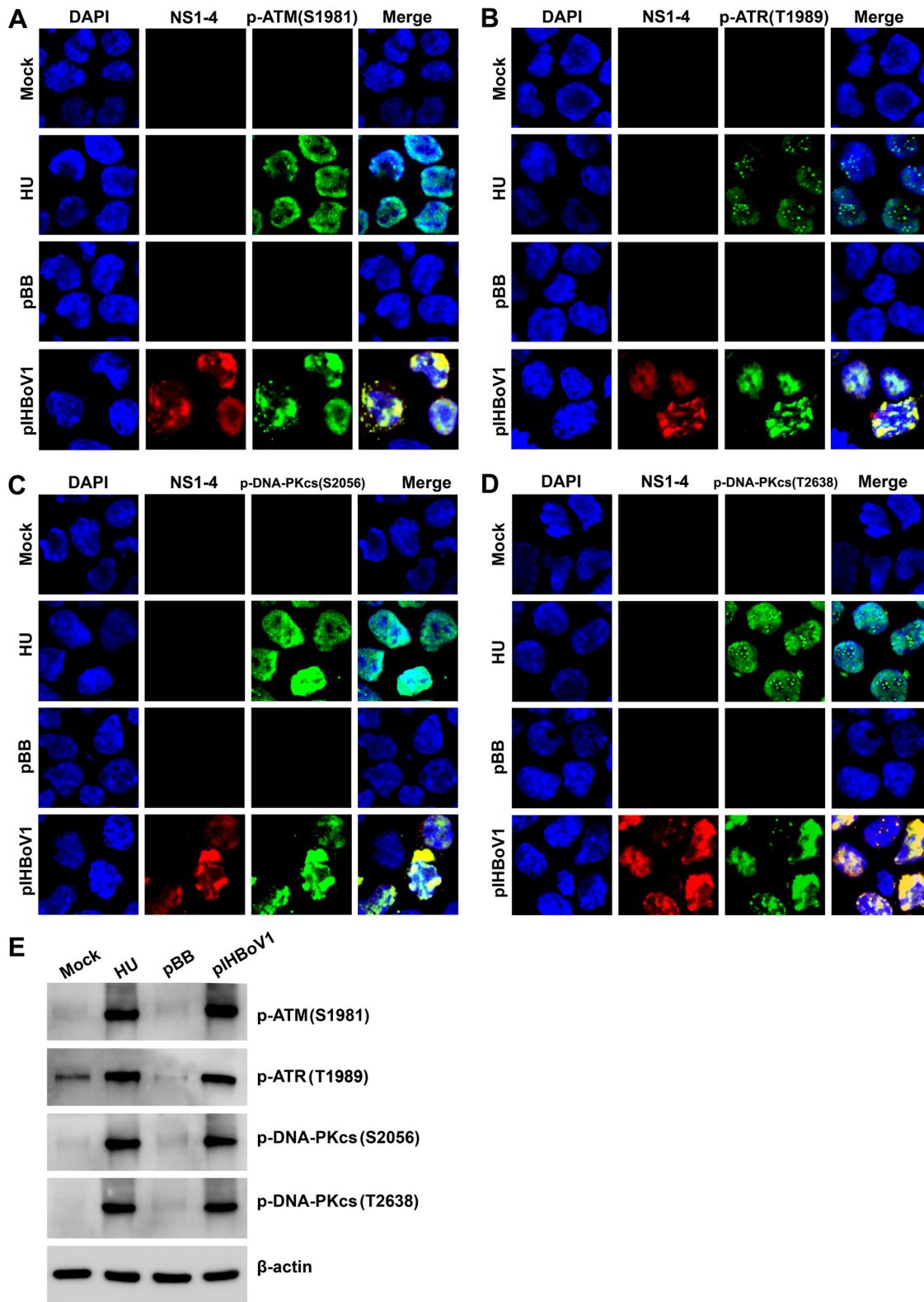


FIG 3 HEK293 cells transfected with pHBoV1 undergo activation of ATM, ATR, and DNA-PKcs. HEK293 cells were transfected with pHBoV1 or pBB. After 2 days, cells were collected for IF and Western blot analyses. HU-treated cells were used as a positive control. (A to D) IF analysis. Cells were collected and costained with anti-NS1C and an antibody against the phosphorylated form of the indicated marker of the DDR. Confocal images were taken at a $\times 100$ magnification. (E) Western blot analysis. Cells were collected and analyzed by Western blotting using an antibody against the phosphorylated form of the indicated marker of the DDR or an anti- β -actin antibody.

damage foci with activated PI3KK colocalized well with the viral DNA replication centers, where the NS proteins were actively expressed and visualized by anti-NS1C antibody. Western blotting confirmed that ATM was phosphorylated at serine 1981 [p-ATM(S1981)] (46), ATR was phosphorylated at threonine 1989 [p-ATR(S1989)] (47), and DNA-PKcs was phosphorylated at both serine 2056 [p-DNA-PKcs(S2056)] (48) and threonine 2638 [p-DNA-PKcs(T2638)] (49) (Fig. 3E). All of these are phosphorylation sites that transduce DDR signaling (46–49). Phosphorylation in response to treatment with HU was used as a positive control for activating the phosphorylation of these proteins.

Collectively, these results confirmed that pHBoV1 transfection induced a DDR (phosphorylation of RPA32 and H2AX) and activation of ATM, ATR, and DNA-PKcs and that the DNA damage foci (the phosphorylation sites of RPA32, H2AX, ATM, ATR, and DNA-PKcs) were limited to the viral DNA replication centers.

HBoV1 NS1 effectively induces a DDR and activates ATM, ATR, and DNA-PKcs.

Bocaparvovirus MVC proteins NS1, NP1, and VP do not induce a DDR during MVC infection (50). Recently, we identified additional HBoV1 nonstructural proteins: NS2, NS3, and NS4 (25). We constructed a series of lentiviral vectors that express each of these nonstructural proteins individually, as well as one that expresses HBoV1 VP proteins, and used them to examine the roles of the respective viral proteins in inducing DDR signaling. Only cells that expressed either NS1 or NS1-70 (and not those expressing green fluorescent protein [GFP], NS2, NS3, NS4, NP1, or VP) were positive for γ H2AX and p-RPA32 staining (Fig. 4). Western blot analysis also demonstrated that p-RPA32 and γ H2AX were present in cells expressing NS1 or NS1-70 or treated with HU but not in cells expressing NS2, NS3, NS4, NP1, or VP (Fig. 5). More importantly, both the IF assay (Fig. 6A to D) and Western blotting (Fig. 6E) showed that cells expressing NS1 or NS1-70 also expressed p-ATM(S1981), p-ATR(S1989), p-DNA-PKcs(S2056), and p-DNA-PKcs(T2638).

Collectively, these data demonstrate that ectopic expression of NS1 or its short variant, NS1-70, is sufficient to induce the phosphorylation of H2AX and RPA32, as well as the activation of ATM, ATR, and DNA-PKcs. Of note, NS1 colocalized with the DNA damage foci marked with the expression of γ H2AX and p-RPA32 (Fig. 4, NS1 and NS1-70) and p-ATM(S1981), p-ATR(S1989), and p-DNA-PKcs(S2056/T2638) (Fig. 6A to D).

To observe whether the NS1-induced DDR was a secondary consequence of cellular chromosome DNA damage, we performed a Comet assay. The Comet assay is a sensitive procedure based on single-cell gel electrophoresis that can detect chromosome DNA damage at the level of the individual eukaryotic cell with a sensitivity of \sim 50 strand breaks per cell (51). This experiment revealed that NS1 expression did not cause extensive damage to cellular DNA. In contrast to the H₂O₂ treatment group, where 100% of cells exhibited signs of DNA damage on electrophoresis and fluorescence staining (DNA fragments from damaged cellular chromosomes migrated away from the nucleus), in the cases of cell transduced with NS1-70 or NS1 (Fig. 7A), very few cells were positive for Comet tails (Fig. 7B and C). Furthermore, we performed a terminal deoxynucleotidyltransferase (TdT)-mediated dUTP-biotin nick end labeling (TUNEL) assay to detect the broken DNA ends of the damaged chromosome. As seen in Fig. 7D and E, transduction of NS1- or NS1-70-expressing lentivirus did not lead to a significant amount of detectable broken DNA ends (less than 2%) compared with that in the mock-transduced group. However, control studies with HU treatment led to severe damage of the cellular DNA (15% TUNEL-positive cells). These results strongly suggest that the expressed NS1 or NS1-70 protein and not a second effector (i.e., damaged cellular DNA) induces DDR signaling.

Both knockdown of ATM, ATR, or DNA-PKcs and inhibition of their phosphorylation impair replication of viral DNA. We next applied ATM-, ATR-, or DNA-PKcs-specific pharmacological inhibitors to HEK293 cells prior to transfection with pHBoV1 and examined the requirement for PI3KK phosphorylation in facilitating the replication of the HBoV1 DNA. Application of the ATM-specific inhibitor KU60019 at a concentration of 5 μ M, the ATR-specific inhibitor VE821 at 2 μ M, and the DNA-PKcs-specific

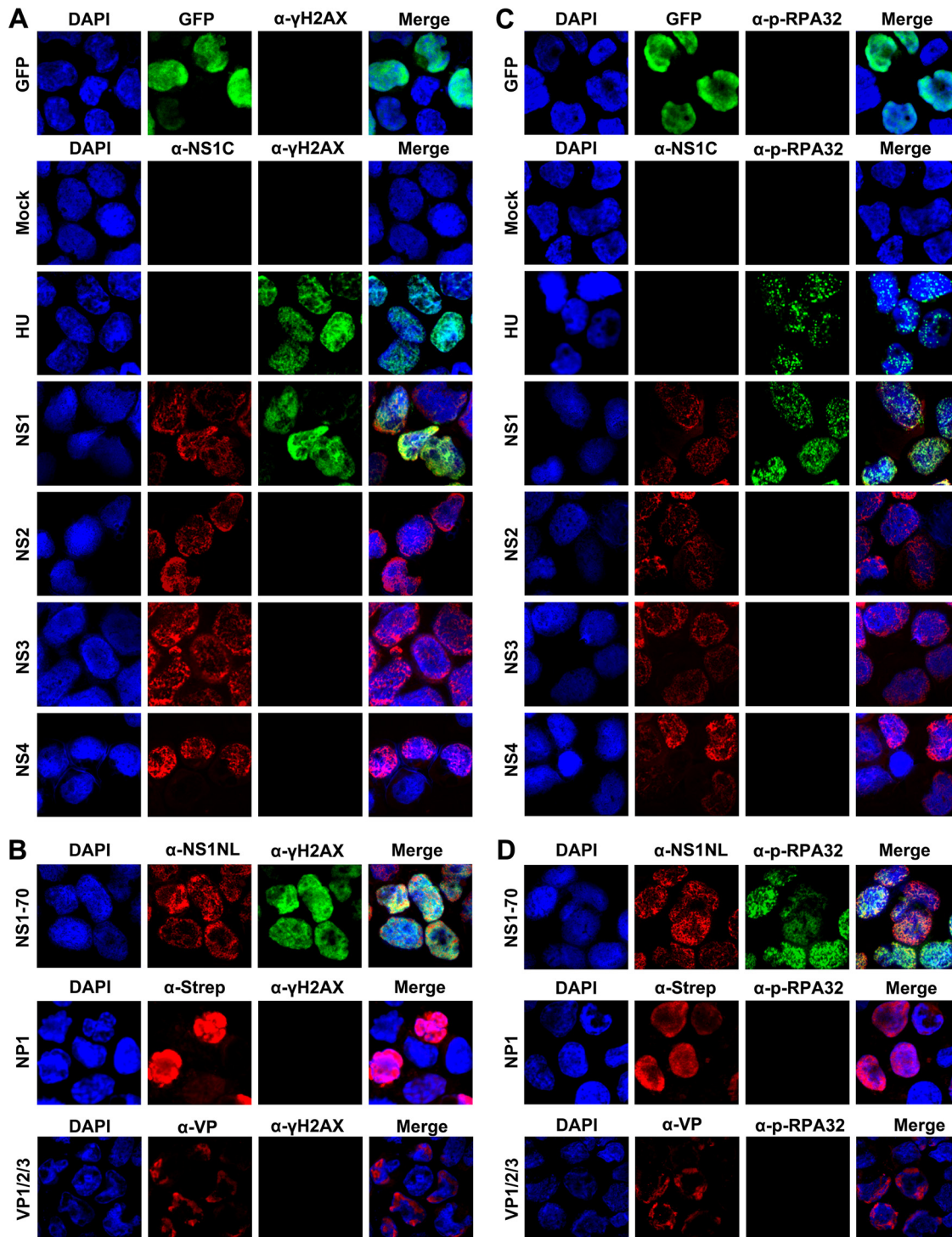


FIG 4 IF analyses of HBoV1 NS1-induced DDR in HEK293 cells. HEK293 cells were transduced with lentiviruses encoding viral NS1, NS1-70, NS2, NS3, NS4, NP1, and VP or GFP (control). At 48 h posttransduction, cells were collected for IF analysis. (A and B) Cells were costained with anti- γ H2AX and anti-NS1C (A) or with anti- γ H2AX and anti-NS1NL, anti-Strep, or anti-VP (B), as indicated. (C and D) Cells were costained with anti-p-RPA32 and anti-NS1C (C) and with anti-p-RPA32 and anti-NS1NL, anti-Strep, or anti-VP (D), as indicated. Nuclei were stained with DAPI (blue). Confocal images were taken at a $\times 100$ magnification. GFP was used as control without staining.

inhibitor NU7441 at $1 \mu\text{M}$ led to decreased HBoV1 DNA replication, with the decreases in the level of the monomeric replicated form (mRF) of the DNA being greater than 10.3-, 25.3-, and 12.5-fold, respectively (Fig. 8A and B). Notably, application of the inhibitors also significantly decreased the levels of production of progeny virions by

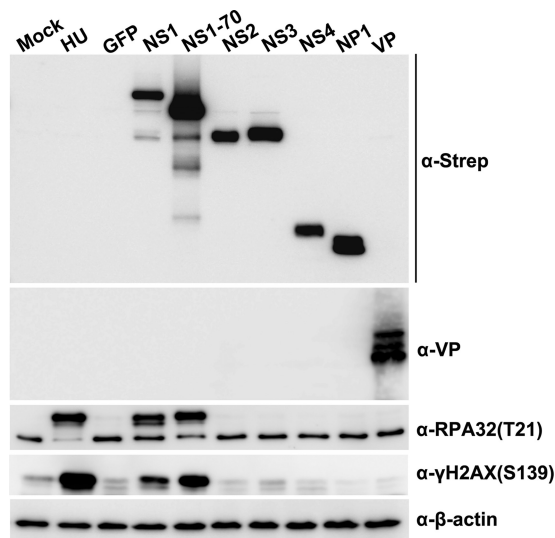


FIG 5 Analyses of HBoV1 NS1-induced DDR in HEK293 cells by Western blotting. Western blotting of HEK293 cells transduced with lentiviruses encoding NS1, NS1-70, NS2, NS3, NS4, NP1, VP, or GFP (control) was performed. At 48 h posttransduction, cell lysates were blotted with anti-Strep, anti-HBoV1 VP, anti-p-RPA32(T21), or anti- γ H2AX(S139) antibody, as indicated. β -Actin was used as a loading control.

over 2 log units (Fig. 8C). As expected, the application of the three inhibitors resulted in an obvious decrease in the levels of γ H2AX and p-RPA32 expression (Fig. 8D). KU60019, VE821, and NU7441 remarkably inhibited the phosphorylation of ATM, ATR, and DNA-PKcs, respectively, but did not alter the level of phosphorylation across targets (Fig. 8E). These results suggest that inhibition of PI3KK activation has a negative effect on HBoV1 DNA replication and the production of progeny virions in HEK293 cells.

To validate the function of ATM, ATR, and DNA-PKcs in the replication of HBoV1 DNA, we used ATR-, ATM-, and DNA-PKcs-specific short hairpin RNAs (shRNAs) to knock down ATR, ATM, and DNA-PKcs, respectively. shRNA-expressing lentiviruses that have been shown to knock down the expression of ATR-, ATM-, or DNA-PKcs successfully (35) were transduced into HEK293 cells prior to the transfection of pIHBoV1. The transduction of each gene-specific shRNA reduced the level of phosphorylation of the PI3KK that it targeted, ATR, ATM, or DNA-PKcs, to the background level in the untransfected (mock-transfected) cells, but the transduction of each gene-specific shRNA did not affect the phosphorylation of the other two PI3KKs (Fig. 9A). The scrambled shRNA (shScram)-transduced control did not reduce the level of phosphorylation, which remained the same as that in the nontransduced (control) cells (Fig. 9A). Southern blot analysis showed that the level of replication of HBoV1 DNA in the ATM-, ATR-, and DNA-PKcs-knockdown HEK293 cells was significantly decreased, with the levels of mRF DNA being reduced 4.3-, 7.4-, and 7.2-fold, respectively (Fig. 9B and C). Consistent with these findings, the ATM-, ATR-, or DNA-PKcs-specific shRNAs (shATM, shATR, and shDNA-PKcs, respectively) reduced the levels of progeny virions by 1.37, 1.79, and 1.86 log units, respectively (Fig. 9D).

Taken together, these results confirmed that the activation of ATM, ATR, and DNA-PKcs individually contributes to the DDR (phosphorylation of H2AX and RPA32) and independently plays an important role in the replication of the HBoV1 duplex genome and in the production of progeny virions in HEK293 cells.

The HBoV1-induced DDR does not cause cell cycle arrest. We previously showed that the DDR induced by infection with bocaparvovirus MVC facilitates replication of the viral DNA by triggering ATM-SMC1-mediated arrest during intra-S phase, which is conducive to the replication of viral DNA (39, 50), because S phase is required for the replication of autonomous parvoviruses in dividing cells (36–38, 41, 42). Thus, we asked whether DDR-facilitated replication of the HBoV1 DNA in HEK293 cells involves S-phase

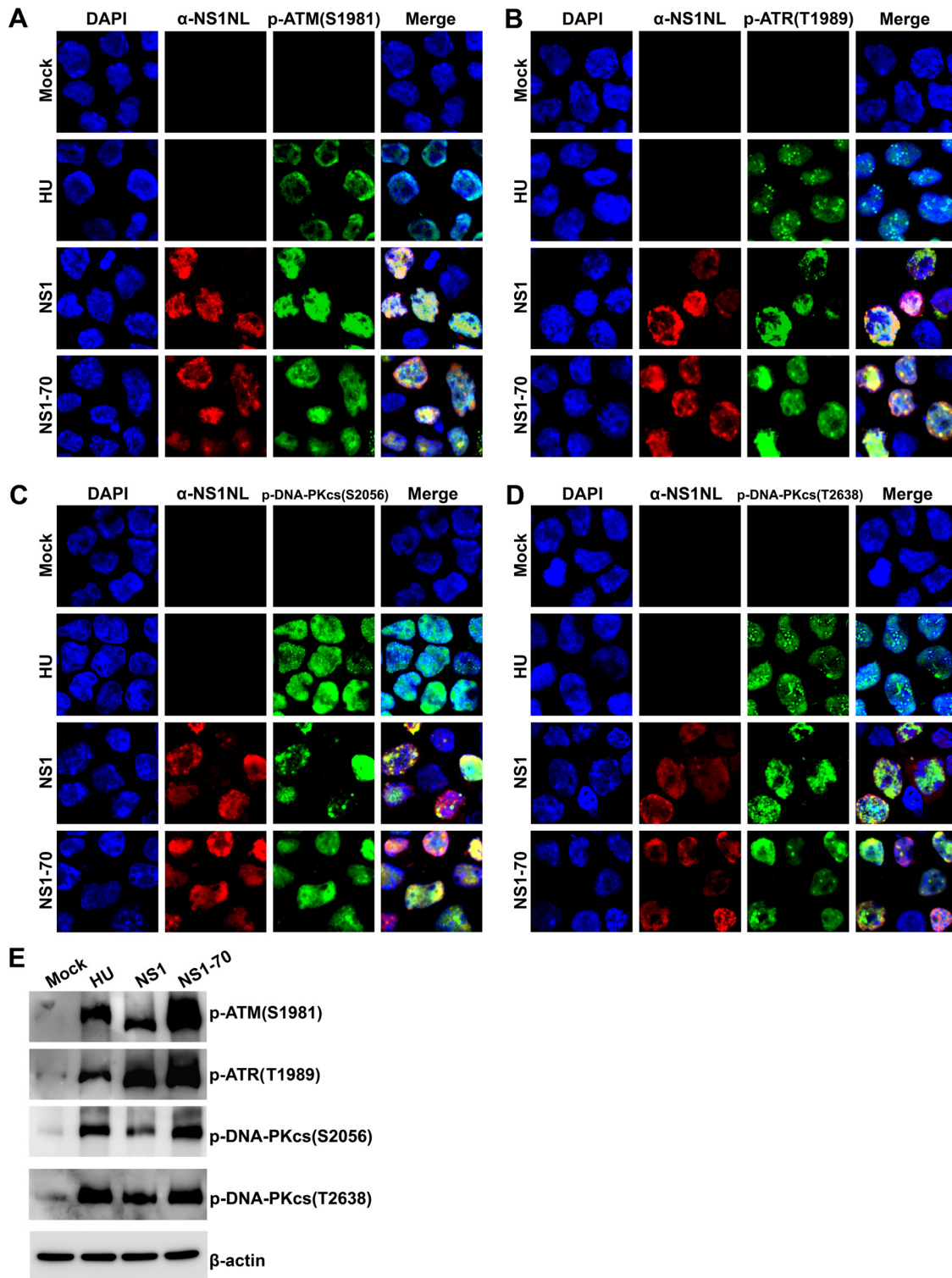


FIG 6 HBoV1 NS1 and NS1-70 activate ATM, ATR, and DNA-PKcs. HEK293 cells were transduced with lentiviruses encoding HBoV1 NS1 or NS1-70. At 48 h posttransduction, they were collected for IF and Western blot analyses. (A to D) IF analysis. Cells were costained with anti-NS1NL antibody (red) and either anti-p-ATM(S1981) antibody (green) (A), anti-p-ATR(T1989) antibody (green) (B), anti-p-DNA-PKcs(S2056) antibody (green) (C), or anti-p-DNA-PKcs(T2638) antibody (green) (D). HU-treated cells were used as a positive control for DDR induction. Nuclei were stained with DAPI (blue). Confocal images were taken at a $\times 100$ magnification. (E) Western blotting. Western blot analysis of mock- or HBoV1 NS1- and NS1-70-transduced cells was performed using anti-p-ATM(S1981), anti-p-ATR(T1989), anti-p-DNA-PKcs(S2056), or anti-p-DNA-PKcs(T2638) antibody. β -Actin served as a loading control.

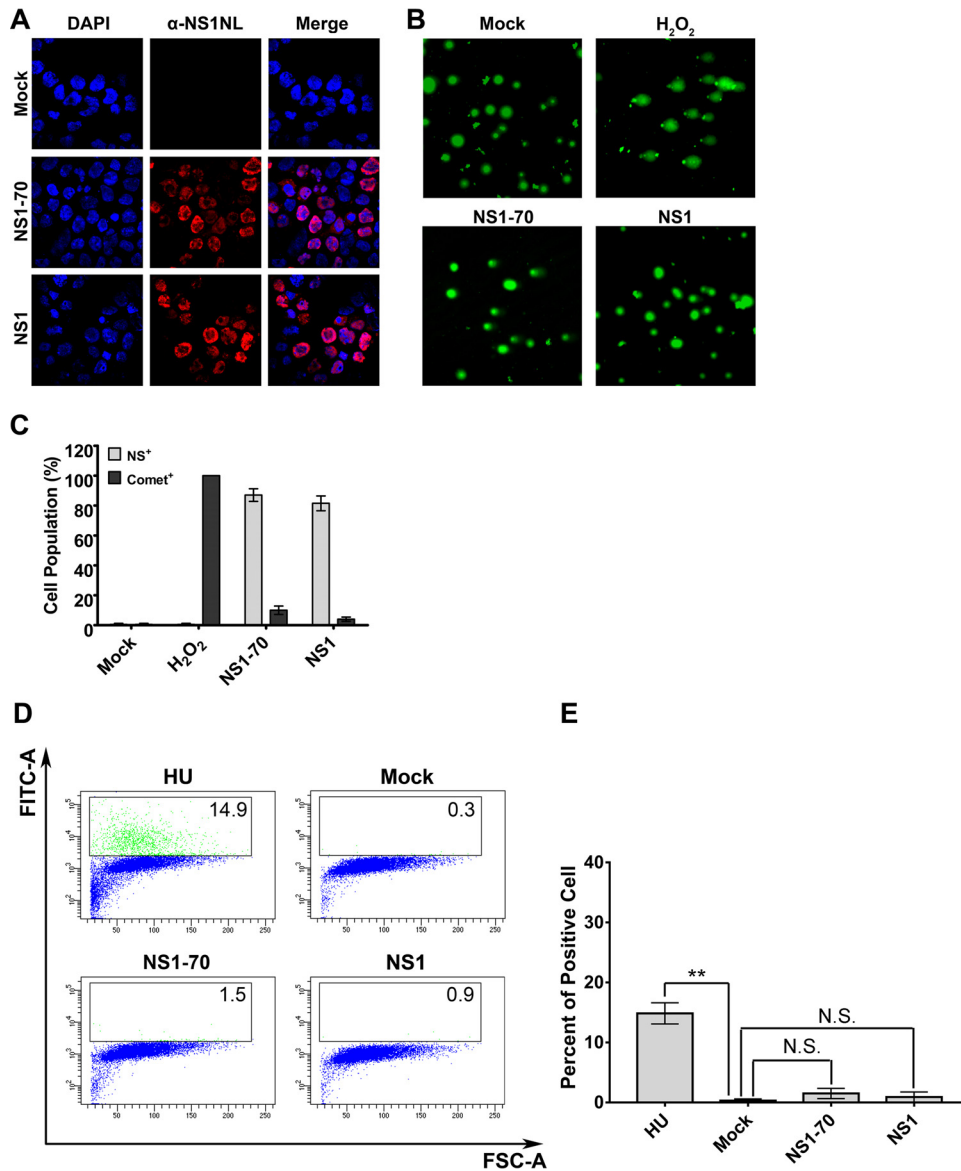


FIG 7 HBov1 NS1 and NS1-70 do not induce significant cellular DNA damage. (A to C) Comet assay. HEK293 cells were transduced with HBov1 NS1- or NS1-70-expressing lentivirus. H₂O₂ treatment was used as a positive control. At 48 h posttransduction, cells were collected for IF analysis and the Comet assay. (A) IF analysis. Half of the cells were stained with anti-HBov1 NS1NL antibody (red). Nuclei were stained with DAPI (blue). Confocal images were taken at a $\times 100$ magnification. (B) Comet assay. The remaining cells were analyzed for damaged DNA using the Comet assay. Confocal images were taken at a magnification of $\times 40$. (C) Quantification of Comet assay results. Statistical analysis of the percentage of cells that contained damaged DNA and were positive for NS1NL (Comet⁺) on the basis of the results three independent experiments was performed. Data are shown as means \pm standard deviations. (D and E) TUNEL assay. (D) HEK293 cells were mock transduced or transduced with HBov1 NS1- or NS1-70-expressing lentivirus. At 48 h posttransduction, HU-treated cells and the transduced cells were collected and the TUNEL assay was performed, followed by flow cytometry. FITC, fluorescein isothiocyanate; FSC, forward scatter. (E) The percentages of TUNEL-positive cells in each group were quantified and are shown as averages and standard deviations, which were generated from three independent experiments. *P* values were calculated using Student's *t* test (**, *P* < 0.01; N.S., no statistically significant difference [*P* > 0.1]).

arrest. Treatment with a pharmacological inhibitor of ATM, ATR, or DNA-PKcs decreased the numbers of NS1-expressing cells by at least 3-fold at 48 h posttransfection (Fig. 10A), consistent with the decrease in the level of mRF DNA (Fig. 8). In untransfected control cells, inhibitor treatment did not obviously affect cell viability (data not shown). Importantly, when cells were transfected with pHBoV1, the numbers of NS-expressing cells in any phase of the cell cycle were similar to those in both mock-transfected cells and cells transfected with the empty vector (pBB) at 48 h (Fig. 10B). In all treated

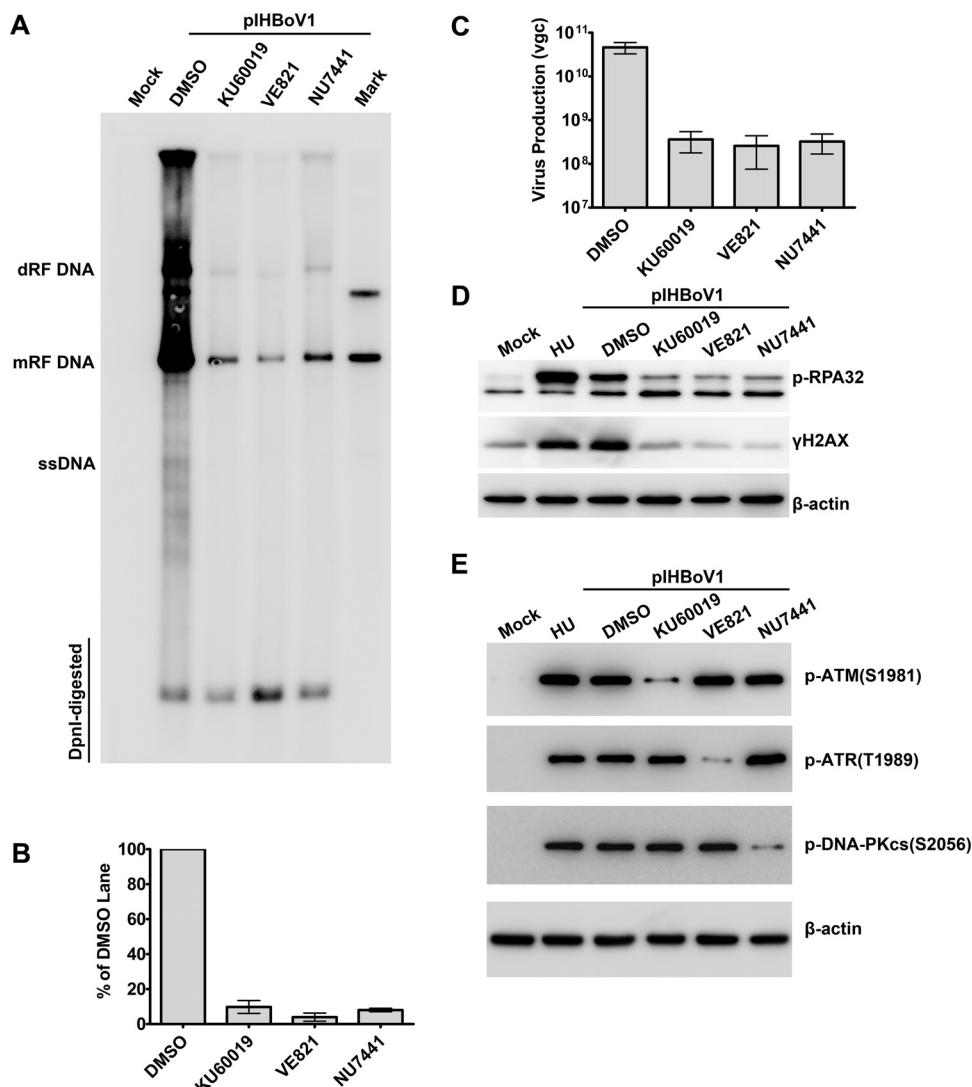


FIG 8 Inhibition of phosphorylation of ATM, ATR, or DNA-PKcs significantly impairs replication of the HBoV1 DNA. HEK293 cells were treated with DMSO or the indicated inhibitor for 4 h prior to transfection with pHBoV1. At 48 h posttransfection, cells were collected for Southern and Western blot analyses. HU-treated cells were used as a positive control for DDR induction. (A and B) Southern blotting. (A) Representative Southern blot of Hirt extracts probed for HBoV1 NS and Cap. The detected bands are labeled as follows: dRF, double replicative form; mRF, monomer replicative form; and ssDNA, single-stranded DNA. (B) Quantification of mRF DNA in the blot following normalization to the amount of DpnI-digested DNA. The data are based on the results of three independent experiments. Means and standard deviations are shown. (C) Quantification of progeny virus produced. Virus was purified from HEK293 cells transfected with pHBoV1 for 48 h. Shown are the average numbers of vgc of purified progeny virions per preparation and standard deviations. (D and E) Western blot analysis. (D) Cell lysates were blotted using anti-p-RPA32. The blot was reblotted with anti-γH2AX and β-actin, in that order. (E) Cell lysates were blotted using anti-p-ATM(S1981), anti-p-ATR(T1989), anti-p-DNA-PKcs(S2056), and β-actin.

groups, as well as in the mock-transfected cells, nearly half of the transfected cells were in S phase. Moreover, NS1-expressing HEK293 cells did not exhibit cell cycle arrest at 9 days and 21 days posttransduction (data not shown).

Taken together, these results confirmed that replication of the duplex HBoV1 genome or NS1 expression did not arrest the cell cycle, suggesting that DDR signaling-facilitated HBoV1 DNA replication is not mediated through an S-phase arrest.

S-phase factors and DNA repair DNA polymerases are recruited into centers of viral DNA replication. Since S-phase arrest was not observed in cells replicating the HBoV1 DNA (Fig. 10), we investigated the role of the S phase in the replication of HBoV1 DNA. We examined the localization of key S-phase (DNA replication) factors, including proliferating cell nuclear antigen (PCNA), replication factor C1 (RFC1), polymerase α (Pol

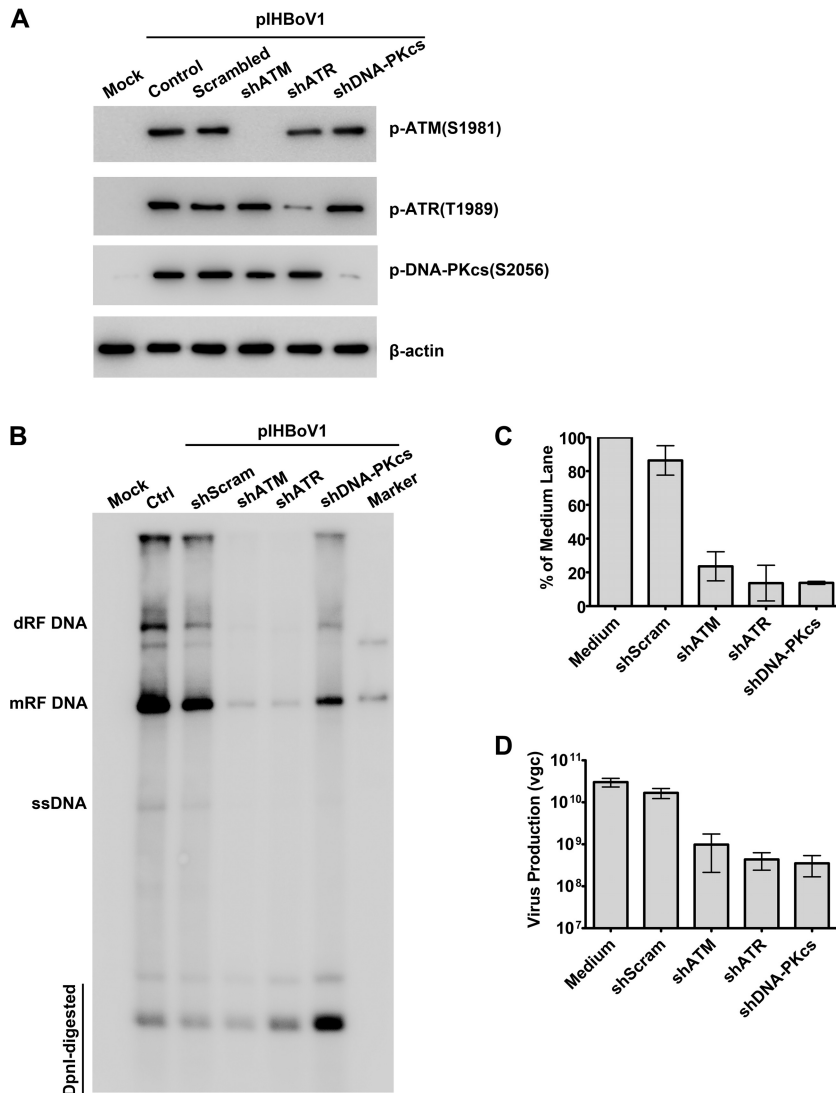


FIG 9 Knockdown of ATM, ATR, or DNA-PKcs significantly decreases the replication of HBoV1 DNA. HEK293 cells were transfected with kinase-targeted shRNAs prior to transfection with pHBoV1. After 2 days, cells were collected. (A) Western blot analysis. The collected cells were analyzed by Western blotting using anti-p-ATM(S1981), anti-p-ATR(T1989), and anti-p-DNA-PKcs(S2056) antibodies, and β -actin was used as a loading control. (B and C) Southern blot analysis. Transfected cells were collected for Hirt DNA extraction and probed for HBoV1 NS and Cap. (B) A representative blot is shown. Ctrl, control. (C) The level of mRF DNA in the blot was quantified and normalized to the level of DpnI-digested DNA from three independent experiments. (D) Progeny virion production. HEK293 cells were treated with DMSO or the indicated inhibitor for 4 h prior to transfection with pHBoV1. At 48 h posttransfection, cells were harvested for virus purification. Averages of the numbers of vgc per preparation with standard deviations are shown.

α), polymerase δ (Pol δ), and polymerase ϵ (Pol ϵ), since all of these proteins have been reported to colocalize in the parvoviral DNA replication centers and to play important roles in the replication of parvovirus DNA (36, 37, 52, 53). We found that PCNA, RPA32, RFC1, Pol α , Pol ϵ , and Pol δ all colocalized with bromodeoxyuridine (BrdU)-labeled viral DNA replication centers in the nucleus (Fig. 11A), as shown by proximity ligation assay (PLA) analysis with antibodies against BrdU and any one of six S-phase factors. PLA amplifies signals when two molecules are within 20 nm of one another (54).

In contrast to replication of the HBoV1 DNA in HEK293 cells, genome replication during the infection of HAE-ALI cultures requires cellular DNA repair DNA polymerases, because S-phase factors are not expressed in differentiated cells (35). Thus, we repeated the colocalization experiment described above but evaluated the colocalization of

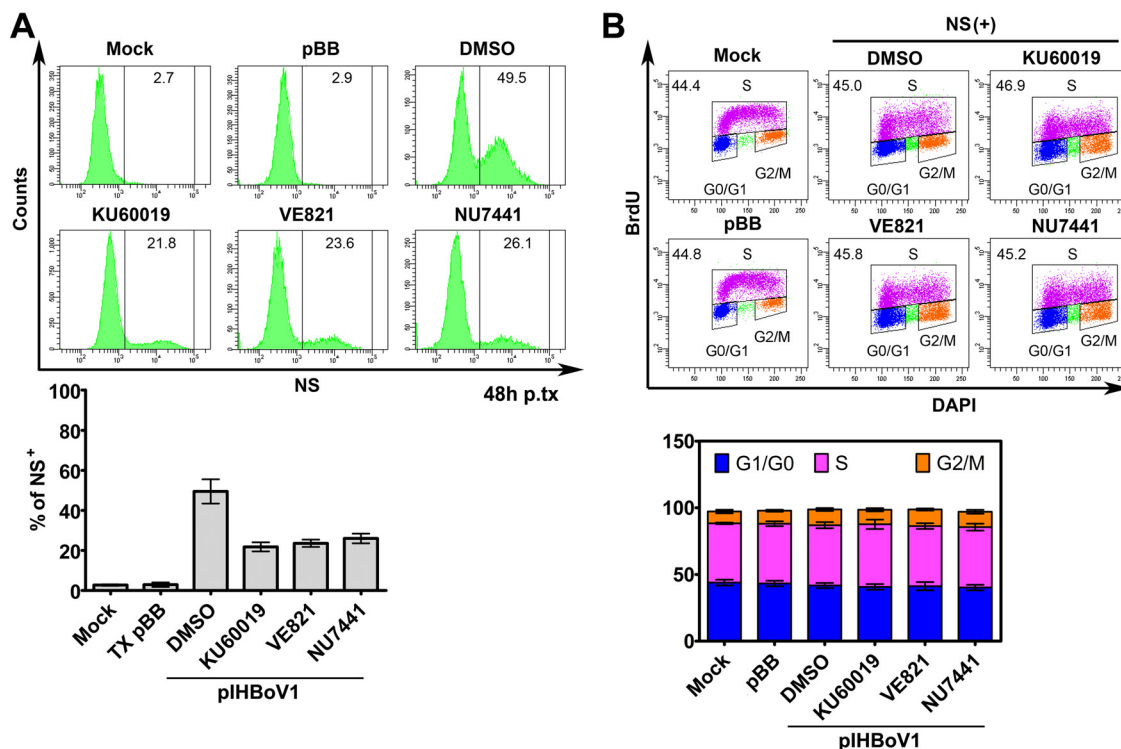


FIG 10 pHBoV1-induced DDR signaling did not cause cell cycle arrest. HEK293 cells were treated with DMSO and the indicated inhibitors for 4 h prior to transfection with pHBoV1. Cell cycle analysis was performed at 48 h posttransfection, following costaining with DAPI, anti-BrdU, and anti-NS1C antibodies. pBB-transfected cells were used as transfection controls. (A) (Top) Flow cytometry analysis of NS expression. (Bottom) NS-expressing cells were analyzed, and the percentage of NS1-expressing cells (NS⁺) after each treatment was plotted. Averages and standard deviations are shown. p.tx, posttransfection; TX, transfection. (B) (Top) Cell cycle analysis. (Bottom) The percentage of cells in each phase was quantified, and the data are shown as means and standard deviations. Each data set was generated from at least three independent experiments.

major DNA repair DNA polymerases with BrdU. Notably, Pol η and Pol κ (DNA polymerases of the Y family), Pol β and Pol λ (DNA polymerases of the X family), and Pol ζ and Rev 1 (DNA polymerases of the B family) colocalized with the BrdU-labeled viral genome, but Pol ι and Pol μ did not (Fig. 11B). As Pol η and Pol κ have been proven to be critical for HBoV1 replication in infected HAE-ALI cultures (35) and they demonstrate high fidelity in DNA repair under certain circumstances (55), we investigated their involvement in HBoV1 DNA replication in HEK293 cells. We used specific shRNAs to selectively knock down their expression. The results showed that the knockdown of either Pol η or Pol κ decreased the level of mRF DNA by >4-fold (Fig. 12A and B).

Taken together, the results of these experiments confirm that both key S-phase DNA replication factors and major DNA repair DNA polymerases are recruited to the viral DNA replication centers and that Y-family DNA polymerases Pol η and Pol κ play an important role during replication of the HBoV1 duplex genome in HEK293 cells.

DISCUSSION

In this study, we discovered that both the replication of the duplex HBoV1 genome and NS1 expression are responsible for inducing DDR through activation of ATM, ATR, and DNA-PKcs. This DDR plays a critical role in the replication of the duplex genome and the production of progeny virions in the absence of cell cycle arrest. We discovered that both S-phase (DNA replication) factors and DNA repair DNA polymerases are recruited to the centers of viral DNA replication and that the Y-family DNA polymerases Pol η and Pol κ play an important role in this process. Thus, our study identifies a unique feature of the parvovirus-induced DDR in dividing cells, i.e., an ability to circumvent the need for cell cycle arrest.

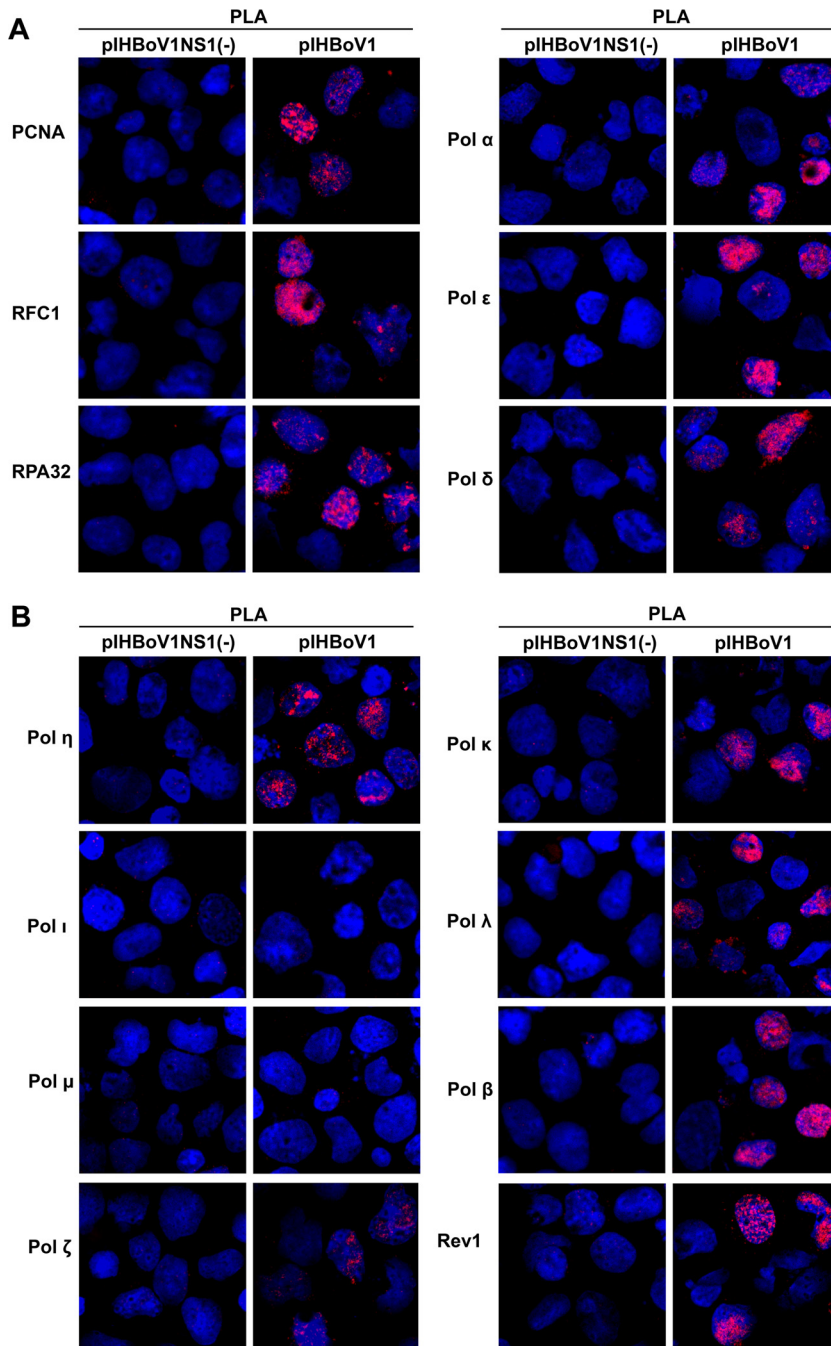


FIG 11 PLA analysis of the S-phase factors DNA repair DNA polymerases with replicating viral DNA. HEK293 cells were transfected with pIHBoV1NS1(-) or pIHBoV1. At 48 h posttransfection they were labeled with BrdU. Cells were cytospun onto slides and were costained with anti-BrdU and anti-PCNA, anti-RFC1, anti-RPA32, anti-Pol δ , anti-Pol α , or anti-Pol ϵ , as indicated (A), or were costained with anti-BrdU and one of the following repair proteins: Pol η , Pol ι , Pol μ , Pol κ , Pol λ , Pol β , Rev 1, or Pol ξ (B). The PLA-amplified signal is shown in red. Nuclei were stained with DAPI (blue). Confocal images were taken at a $\times 100$ magnification.

We previously found that although the NS2 to NS4 proteins are dispensable for both the replication of viral DNA and the production of virions in HEK293 cells, NS2 plays a critical role in the replication of HBoV1 DNA in HAE-ALI cultures (25). The NS2 to NS4 proteins contain a subset of the predicted domains in NS1: OBD and TAD, helicase and TAD, and TAD, respectively (25). Likewise, NS1-70 contains only the OBD and helicase domains of NS1. However, like NS1, NS1-70 is able to induce DDR signaling. This

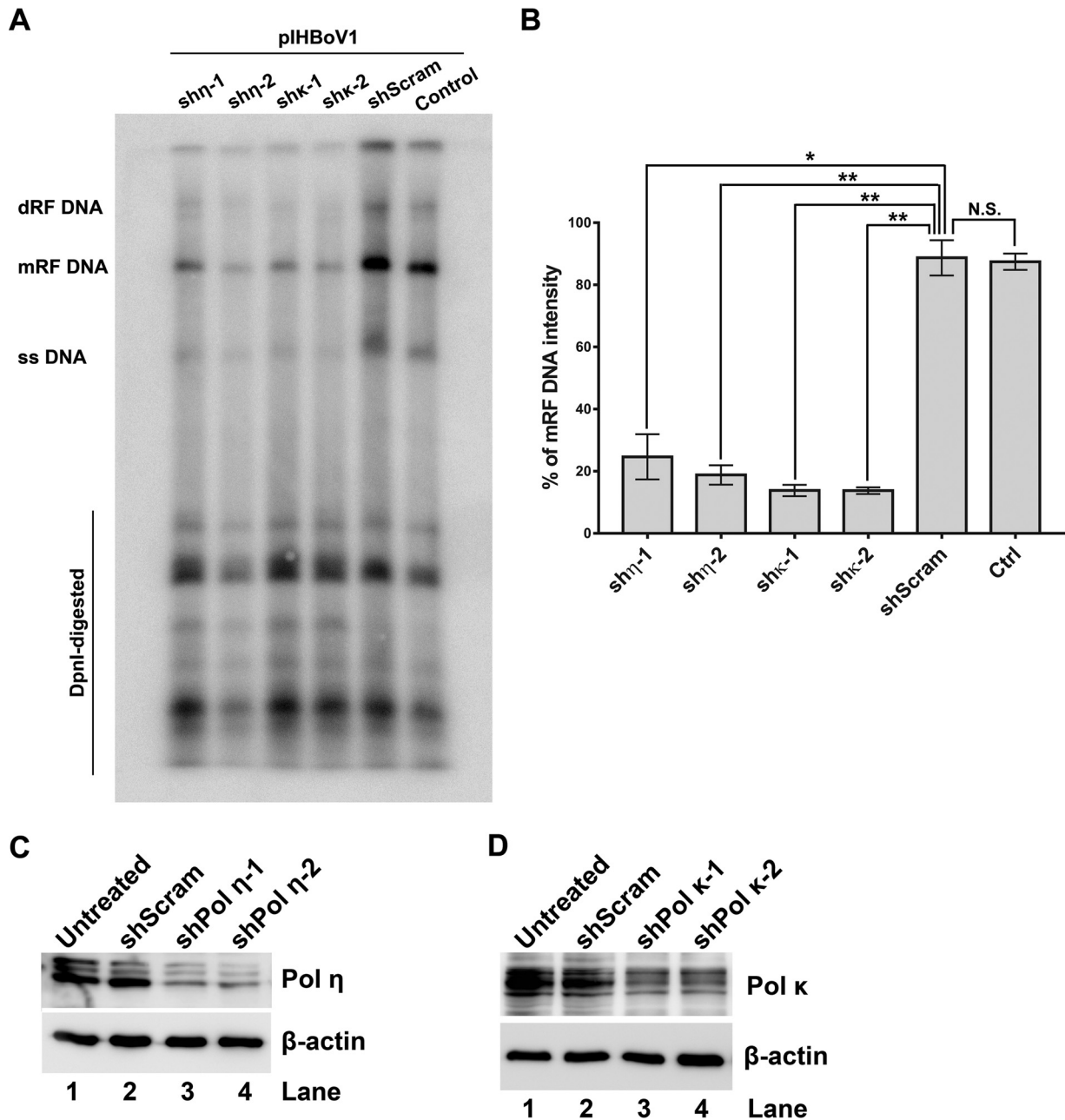


FIG 12 Knockdown of DNA repair DNA polymerase η or κ decreases HBoV1 DNA replication significantly. HEK293 cells were transduced with Pol η - or Pol κ -specific shRNA, as indicated, prior to pIHBoV1 transfection. (A and B) Southern blot analysis. At 48 h posttransfection, cells were collected for Hirt DNA extraction. (A) Hirt DNA samples were digested with DpnI and were subjected to Southern blotting using a probe spanning the HBoV1 NS and Cap genes. A representative blot is shown. (B) The levels of mRF DNA in the blot were quantified and normalized to the level of the control group without shRNA application. Means and standard deviations calculated from three independent experiments are shown. *P* values were calculated using Student's *t* test (*, *P* < 0.05; **, *P* < 0.01; N.S., no statistically significant difference [*P* > 0.1]). (C and D) Western blot analysis. At 48 h posttransfection, cells were collected and the cell lysates were analyzed for the expression of Pol η (C) and Pol κ (D). β -Actin was also probed as a loading control.

suggests that both OBD and the helicase domain are required to induce a DDR. A mutant infectious clone that expresses only NS1-70 replicates in HEK293 cells, though to a lesser extent (~10-fold) than in wild-type cells (data not shown). Thus, the C-terminal TAD of NS1 may serve as a facilitator for replication of the HBoV1 DNA. Notably, NS1-70 is barely expressed in HEK293 cells transfected with pIHBoV1 but is present at higher levels during virus infection of HAE-ALI cultures (25). This finding supports the notion that the DDR induced by NS1-70 plays a role in virus infection of HAE-ALI cultures.

The NS1 proteins of parvoviruses are multifunctional. They bind the viral origin of replication, nick viral DNA (56), and play an important role in inducing apoptosis and cell cycle arrest (57). However, HBoV1 NS1 is the only parvovirus NS1 protein that has been reported to activate ATM, ATR, and DNA-PKcs and to induce hallmarks of DDR (58, 59). The conventional cellular response to DNA damage involves signaling events initiated by damage to the cellular genome (60). Many DNA viruses induce DDR signaling during infection through a response that is initiated by incoming viral DNA or by replicating genomes, virus infection-caused damage of cellular DNA, and viral proteins (61). More importantly, viral proteins can directly bind to and activate cellular DDR factors without damaging chromosome DNA (61). For examples, the M2 protein of murine gammaherpesvirus 68 (MHV68) binds directly to ATM and induces ATM kinase activation in the absence of DNA damage (62). Similarly, the Tax oncoprotein of human T lymphotropic virus type 1 (HTLV-1) can form pseudo-DDR foci in cells by tethering MDC1 to chromatin and recruiting DDR factors, including γ H2AX and activated DNA-PKcs (63, 64). Additionally, in the conventional cellular response to DNA damage, H2AX phosphorylation is transmitted from the damaged foci throughout the chromosome DNA (65, 66). In contrast, the NS1- or HBoV1 replication-induced H2AX phosphorylation is limited to within NS1-expressing foci and the viral DNA replication centers. Furthermore, no significant broken ends of DNA were observed in NS1-expressing cells that exhibited a DDR (Fig. 7). These lines of evidence support the suggestion that the HBoV1 NS1 protein forms pseudo-DDR foci (DNA damage foci) by recruiting DDR γ H2AX and p-RPA32 and activates ATM, ATR and DNA-PKs without causing cellular chromosome DNA damage; this represents a distinct type of virus-induced damage signaling.

We have previously shown that DNA replication (or the viral replicative intermediates) of the bocaparvovirus MVC induces a DDR, while MVC NS1 does not (50). Thus, it is possible that both HBoV1 NS1 and viral replicative intermediates contribute to the viral DNA replication-induced DDR. However, considering the high degree of similarity between the DDRs induced during HBoV1 DNA replication and by NS1 expression (compare Fig. 2 and 3 with Fig. 4 and 6) and the fact that NS1 expression precedes the replication of duplex DNA in HEK293 cells, we believe that the NS1-induced DDR plays a critical role in HBoV1 DNA replication in HEK293 cells. As DDR signaling is critical to the replication of HBoV1 DNA in both HAE-ALI and HEK293 cells, we hypothesize that HBoV1 NS1 activates three PI3KKs, which in turn phosphorylate H2AX and RPA32. This may confer an evolutionary advantage to HBoV1 by efficiently recruiting the DNA replication and repair factors that are required for viral DNA replication prior to the onset of duplex genome DNA replication within viral DNA replication centers.

Prior to our recent report on HBoV1 replication in differentiated airway epithelial cells (35), it was thought that the replication of autonomous parvoviruses depended on cells being in S phase. Due to the lack of a system that models cell division within an epithelium (22), we used the HBoV1 reverse genetics system to examine the basis of the S-phase requirement during HBoV1 DNA replication in transfected HEK293 cells. Although HBoV1 replication in HEK293 cells induced DDR signaling, this did not trigger arrest of the cell cycle, with a high percentage of transfected cells being in S phase. In other autonomous parvoviruses, the effects of the DDR on DNA replication in dividing cells are largely due to arrest of the cell cycle (59). Infection of Walter Reed/3873D (WRD) canine cells with MVC and *ex vivo*-expanded human primary erythroid progenitor cells with parvovirus B19 has been shown to induce a prolonged S phase, due to the infection-induced DDR (39, 40). In nondividing cells, where S-phase factors are not available, HBoV1 is able to hijack cellular DNA repair DNA polymerases in replicating its genome (35). The involvement of the Y-family DNA polymerases Pol η and Pol κ in amplification of the HBoV1 genome of infected HAE-ALI cultures (35), as well as in HBoV1 DNA replication of HEK293 cells (Fig. 12), suggests that DNA repair is required for viral genome replication. It is surprising that other DNA repair DNA polymerases, such as the X-family Pol β and Pol λ and B-family Pol ζ and Rev 3, also colocalize within the viral DNA replication centers. Meanwhile, S-phase factors PCNA, RPA32, and RFC1, as well as DNA replication polymerases Pol α , Pol ϵ , and Pol δ , are recruited into the viral

centers of DNA replication. We speculate that HBoV1 proteins or DNA are powerful recruiters of the cellular DNA replication and repair machinery. However, the exact functions of these S-phase factors and other DNA repair DNA polymerases (Pol β , Pol λ , Pol ζ , and Rev 3) in HBoV1 DNA replication require further investigation.

In summary, our analysis suggests that HBoV1 has evolved to use NS1 in activating DDR signaling, which in turn results in the recruitment of cellular DNA replication factors and DNA repair polymerases to the viral DNA replication centers. Thus, the HBoV1 genome could potentially replicate using the Y-family DNA polymerases. The same principle may apply to the replication of other bocaparvoviruses in dividing and nondividing cells. One candidate for such a mechanism is MVC, which also replicates in nondividing canine airway epithelial cells (data not shown). It is possible that parvoviruses have evolved a variety of mechanisms to replicate their DNA in host cells.

MATERIALS AND METHODS

Cell culture. HEK293 cells were purchased from the American Type Culture Collection (ATCC; Manassas, VA) and were maintained in Dulbecco's modified Eagle's medium (DMEM; GE Healthcare Bio-Sciences, Piscataway, NJ) with 10% fetal calf serum (FCS; Sigma-Aldrich, St. Louis, MO) at 37°C in 5% CO₂.

Chemicals and treatments. A 200 mM stock of hydroxyurea (HU; Calbiochem, Billerica, MA) was prepared in deionized water (dH₂O). The following pharmacological inhibitors of PI3Ks were used: the ATM-specific inhibitor KU60019 (67) (Tocris Bioscience, Bristol, UK), the ATR-specific inhibitor VE821 (68) (Selleckchem, Houston, TX), and the DNA-PKcs-specific inhibitor NU7441 (69) (Tocris Bioscience). All inhibitors were dissolved in dimethyl sulfoxide (DMSO) as 10 mM stock solutions. A 10 mM stock of bromodeoxyuridine (5-bromo-2'-deoxyuridine [BrdU]; Sigma) was prepared in dH₂O.

HEK293 cells were seeded on 6-well plates 1 day prior to chemical treatment. Inhibitors were applied to cell cultures 4 h prior to transfection, with KU60019, VE821, and NU7441 being added to final concentrations of 5, 2, and 1 μ M, respectively. To treat cells, HU was used at a final concentration of 5 mM.

Transfection. Transfection with viral duplex DNA was performed using the LipoD293 transfection reagent (SignaGen Laboratories, Gaithersburg, MD) or the Lipofectamine and Plus reagents (Invitrogen, Grand Island, NY) according to the manufacturers' instructions.

Plasmid construction. (i) Lentiviral constructs for the production of virus proteins. The open reading frames (ORFs) of the HBoV1 NS1, NP1, and VP proteins were optimized at GenScript USA Inc. (Piscataway, NJ). pLenti-CMV-IRES-GFP-WPRE (70) was used as the vector, and the ORFs of NS1, NS1-70, NS2, NS3, NS4, NP1, and VP1 were inserted into the BamHI and XhoI restriction sites. The C terminus of each of these HBoV1 proteins was fused, in frame, to a streptavidin (Strep) tag; in the case of VP1, the translation initiation site AAG-CAG-AUG was optimized to GUU AAG ACG (where the underlined nucleotides represent the translation initiation codon, nt 3152 of the HBoV1 genome, Genbank accession no. JQ923422) to ensure that VP1, -2, and -3 would be expressed at the native ratio, i.e., 1:1:10 (data not shown).

(ii) pLKO-shRNA constructs. The shRNA-expressing constructs were generated as previously described (71). The following shRNA sequences were chosen for targeting of the genes of interest: an shRNA specific to ATM (shATM), 5'-GAT CCC CGG ATT TGC GTA TTA CTC AGT TCA AGA GAC TGA ATA CGC AAA TCC TTT TTG GAA A-3'; an shRNA specific to ATR (shATR), 5'-GAT CCC CGG CGT CGT CTC AGC TCG TCT TCA AGA GAG ACG AGC TGA GAC GAC GCC TTT TTG GAA A-3'; an shRNA specific to DNA-PKcs (shDNA-PKcs), 5'-CCG GGA TCG CAC CTT ACT CTG TTC TCG AGA ACA GAG TAA GGT GCG ATC TTT TTG-3'; two shRNAs specific to DNA Pol η , 5'-CCG GCC CGC TAT GAT GCT CAC AAG ACT CGA GTC TTG TGA GCA TCA TAG CCG GTT TTT G-3' (shPol η -1) and 5'-CCG GCA GCC AAA TGC CCA TTC CCA ACT CGA GTT GCG AAT GGG CAT TTG GCT GTT TTT G-3' (shPol η -2); two shRNAs specific to DNA Pol κ , 5'-CCG GGC CAT TGC TAA GGA ATT GCT ACT CGA GTA GCA ATT CCT TAG CAA TGG CTT TTT G-3' (shPol κ -1) and 5'-CCG GGC ATT GAT CCT AGT GTC TTT ACT CGA GTA AAG ACA CTA GGA TCA ATG CTT TTT G-3' (shPol κ -2); and a scrambled shRNA (shScram) control, 5'-CCG GCC TAA GGT TAA GTC GCC CTC GCT CGA GCG AGG GCG ACT TAA CCT TAG GTT TTT G-3'.

Lentivirus production and transduction. Lentiviruses were generated, and the transduction unit was determined in HEK293 cells as previously described (72). HEK293 cells were transduced at a multiplicity of infection (MOI) of approximately 5 units per cell.

Virus production. HEK293 cells were cultured on a 145-mm plate, and inhibitors KU60019, VE821 and NU7441 were applied at final concentration of 5, 2, and 1 μ M, respectively, 6 h prior to transfection with pHBoV1. After 2 days, the cells were collected and lysed for virus production, followed by quantification of viral genome copies (vgc) by quantitative PCR (qPCR) as previously described (22).

IF analysis. Immunofluorescence (IF) staining was performed as previously described (73). Briefly, cells were collected and cytospun onto slides. They were then fixed with 3.7% paraformaldehyde (PFA) in phosphate-buffered saline (PBS; pH 7.4) at room temperature for 15 min, washed in PBS three times for 5 min each time, and permeabilized with 0.5% Triton X-100 for 5 min. Primary antibodies were diluted in PBS with 2% FCS. After a 1-h incubation at 37°C, secondary antibodies were applied, followed by staining of the nuclei with DAPI (4',6-diamidino-2-phenylindole). Confocal images were captured using an Eclipse C1 Plus confocal microscope (Nikon) controlled using Nikon EZ-C1 software.

BrdU incorporation (pulse-labeling) assay. BrdU was added to HEK293 cells at a final concentration of 30 μ M, and the cells were incubated for 30 min (39). They were then collected, fixed in 3.7% PFA for 30 min, and permeabilized with 0.5% Triton X-100 for 5 min. Cells were costained with an antibody against BrdU and one against anti-NS1C, a specific cellular S-phase factor, or a specific DNA polymerase, followed by staining with appropriate secondary antibodies or DAPI.

PLA. The proximity ligation assay (PLA; Sigma, St. Louis, MO) was performed as previously described (35), according to the manufacturer's instructions. Briefly, HEK293 cells were labeled with BrdU as described above, and the cells were cytospun onto slides. At room temperature, the cells were fixed with 3.7% PFA for 15 min, permeabilized with 0.2% Triton X-100 for 5 min, and blocked with Duolink blocking buffer for 30 min. The cells were then incubated with primary antibodies against BrdU and anti-PCNA or any other antibodies for 1 h at room temperature. Two diluted PLA probes were applied to the cells, and the mixture was incubated for 1 h at 37°C. Hybridized oligonucleotides were then ligated in the ligation solution for 30 min at 37°C and amplified in the amplification solution for 100 min. The cells were then washed and mounted with Duolink *in situ* mounting medium with DAPI and analyzed by examination under a Nikon Eclipse C1 Plus confocal microscope.

Western blot and Southern blot analyses. Western blotting was performed as previously described (40). For Southern blotting, low-molecular-weight (Hirt) DNA was extracted from pHBoV1-transfected HEK293 cells, and analysis was performed as previously described (25), using an HBoV1 NS and *Cap* gene probe.

Comet assay. A comet assay kit was purchased from Cell Biolabs Inc. (San Diego, CA) and used according to the manufacturer's instructions as previously described (39). Briefly, mock-, NS1-, or NS1-70-transduced cells were trypsinized and diluted in PBS. Untransduced cells were treated with 100 μ M H₂O₂ at 4°C for 20 min and used as positive controls for DNA damage. Mock-, NS1-, and NS1-70-transduced cells as well as H₂O₂-treated cells were mixed with 1% low-melting-point agarose and transferred onto slides. The slides were electrophoresed in alkaline buffer, stained with diluted Vista green dye, and analyzed under a Nikon Eclipse C1 Plus confocal microscope.

TUNEL assay. A terminal deoxynucleotidyltransferase (TdT)-mediated dUTP-biotin nick end labeling (TUNEL) assay was performed according to the manufacturer's instructions (Biotool, Houston, TX). Briefly, HEK293 cells were mock transduced or transduced with an NS-expressing lentivirus vector. At 48 h posttransduction, approximately 1.5×10^6 of the cells from each group were collected and fixed with 3.7% PFA at room temperature for 1 h. After the cells were washed with PBS three times, they were permeabilized in PBS containing 0.2% Triton X-100 for 5 min. Then, the cells were incubated with 100 μ l $1 \times$ equilibration buffer for 5 min, followed by addition of 50 μ l of a reaction mixture that contained the TdT enzyme and Apo-Green labeling solution. After incubation at 37°C for 60 min, the cells were washed with PBS three times, stained with DAPI, and subjected to flow cytometry analysis.

Flow cytometry analysis. For cell cycle analysis, the cells were stained and analyzed by flow cytometry as previously described (39). Briefly, they were incubated with 30 μ M BrdU for 1 h. Collected cells were fixed, permeabilized, and treated with 1 M HCl for 30 min to denature chromosome DNA. The treated cells were costained with anti-BrdU and anti-HBoV1 NS1C antibodies, followed by flow cytometry.

Antibodies used. The following antisera were developed previously: rat anti-HBoV1 NS1C, which recognizes NS1, NS2, NS3, and NS4; anti-HBoV1 VP, which recognizes VP1, VP2, and VP3 (27); and anti-HBoV1 NS1NL, which recognizes NS1, NS2, NS3, NS4, and NS1-70 (25). All other antibodies used in the study were purchased: anti-phosphorylated H2AX and anti- γ -H2AX(Ser139) from Millipore (Billerica, MA); anti-phosphorylated replication protein A32, p-RPA32(Thr21), anti-p-ATR(Thr1989), and anti-Pol ι from GeneTex (Irvine, CA); anti-p-ATM(Ser1981), anti-p-DNA-PKcs(Ser2056), anti-p-DNA-PKcs(Thr2638), anti-Pol η , anti-Pol κ , and anti-Pol ζ from Abcam (Cambridge, MA); anti-Strep from GenScript (Piscataway, NJ); anti-PCNA from Abgent (San Diego, CA); anti-Pol μ from Bioss (Woburn, MA); anti-RFC1, anti-Pol α , anti-Rev 1, anti-Pol δ , and anti-Pol β from Santa Cruz (Dallas, TX); anti-RPA32, anti-Pol ϵ , and anti-Pol λ from Bethyl Laboratories (Montgomery, TX); anti-Ki67 from BD Biosciences (San Jose, CA); anti-BrdU from Rockland (Limerick, PA); and anti- β -actin from Sigma (St. Louis, MO).

ACKNOWLEDGMENTS

We thank members of the J. Qiu lab for valuable discussions.

This study was supported by the following grants: PHS grants AI070723, AI105543, and AI112803 from NIAID, NIH, to J.Q.; a subaward of P30 GM103326 from the COBRE program of NIGMS, NIH, to J.Q.; and award YAN15XX0 from the Cystic Fibrosis Foundation to Z.Y.

The funders had no role in study design, data collection and interpretation, or the decision to submit the work for publication.

REFERENCES

- Allander T, Tammi MT, Eriksson M, Bjerkner A, Tiveljung-Lindell A, Andersson B. 2005. Cloning of a human parvovirus by molecular screening of respiratory tract samples. *Proc Natl Acad Sci U S A* 102:12891–12896. <https://doi.org/10.1073/pnas.0504666102>.
- Cotmore SF, Agbandje-McKenna M, Chiorini JA, Mukha DV, Pintel DJ, Qiu J, Söderlund-Venermo M, Tattersall P, Tijssen P, Gatherer D, Davison AJ. 2014. The family Parvoviridae. *Arch Virol* 159:1239–1247. <https://doi.org/10.1007/s00705-013-1914-1>.
- Dijkman R, Koekkoek SM, Molenkamp R, Schildgen O, van der Hoek L. 2009. Human bocavirus can be cultured in differentiated human airway epithelial cells. *J Virol* 83:7739–7748. <https://doi.org/10.1128/JVI.00614-09>.
- Bates RC, Storz J, Reed DE. 1972. Isolation and comparison of bovine

- parvoviruses. *J Infect Dis* 126:531–536. <https://doi.org/10.1093/infdis/126.5.531>.
5. Binn LN, Lazar EC, Eddy GA, Kajima M. 1970. Recovery and characterization of a minute virus of canines. *Infect Immun* 1:503–508.
 6. Arthur JL, Higgins GD, Davidson GP, Givney RC, Ratcliff RM. 2009. A novel bocavirus associated with acute gastroenteritis in Australian children. *PLoS Pathog* 5:e1000391. <https://doi.org/10.1371/journal.ppat.1000391>.
 7. Cheng WX, Li JS, Huang CP, Yao DP, Liu N, Cui SX, Jin Y, Duan ZJ. 2010. Identification and nearly full-length genome characterization of novel porcine bocaviruses. *PLoS One* 5:e13583. <https://doi.org/10.1371/journal.pone.0013583>.
 8. Kapoor A, Mehta N, Esper F, Poljsak-Prijatelj M, Quan PL, Qaisar N, Delwart E, Lipkin WI. 2010. Identification and characterization of a new bocavirus species in gorillas. *PLoS One* 5:e11948. <https://doi.org/10.1371/journal.pone.0011948>.
 9. Johnson FB, Qiu J. 2011. Bocavirus, Parvoviridae, Parvovirinae, p 1209–1215. *In* Tidona C, Darai G (ed), *The Springer index of viruses*, 2nd ed. Springer, New York, NY.
 10. Allander T, Jartti T, Gupta S, Niesters HG, Lehtinen P, Osterback R, Vuorinen T, Waris M, Bjerkner A, Tiveljung-Lindell A, van den Hoogen BG, Hyypää T, Ruuskanen O. 2007. Human bocavirus and acute wheezing in children. *Clin Infect Dis* 44:904–910. <https://doi.org/10.1086/512196>.
 11. Gendrel D, Guedj R, Pons-Catalano C, Emirani A, Raymond J, Rozenberg F, Lebon P. 2007. Human bocavirus in children with acute asthma. *Clin Infect Dis* 45:404–405. <https://doi.org/10.1086/519505>.
 12. Kahn J. 2008. Human bocavirus: clinical significance and implications. *Curr Opin Pediatr* 20:62–66. <https://doi.org/10.1097/MOP.0b013e3282f3f518>.
 13. Schildgen O, Muller A, Allander T, Mackay IM, Volz S, Kupfer B, Simon A. 2008. Human bocavirus: passenger or pathogen in acute respiratory tract infections? *Clin Microbiol Rev* 21:291–304. <https://doi.org/10.1128/CMR.00030-07>.
 14. Martin ET, Fairchok MP, Kuypers J, Magaret A, Zerr DM, Wald A, Englund JA. 2010. Frequent and prolonged shedding of bocavirus in young children attending daycare. *J Infect Dis* 201:1625–1632. <https://doi.org/10.1086/652405>.
 15. Garcia-Garcia ML, Calvo C, Falcon A, Pozo F, Perez-Brena P, De Ca JM, Casas I. 2010. Role of emerging respiratory viruses in children with severe acute wheezing. *Pediatr Pulmonol* 45:585–591. <https://doi.org/10.1002/ppul.21225>.
 16. Don M, Söderlund-Venermo M, Valent F, Lahtinen A, Hedman L, Canciani M, Hedman K, Korppi M. 2010. Serologically verified human bocavirus pneumonia in children. *Pediatr Pulmonol* 45:120–126. <https://doi.org/10.1002/ppul.21151>.
 17. Proenca-Modena JL, Gagliardi TB, Escremim de PF, Iwamoto MA, Criado MF, Camara AA, Acrani GO, Cintra OA, Cervi MC, de Paula Arruda LK, Arruda E. 2011. Detection of human bocavirus mRNA in respiratory secretions correlates with high viral load and concurrent diarrhea. *PLoS One* 6:e21083. <https://doi.org/10.1371/journal.pone.0021083>.
 18. Jartti T, Hedman K, Jartti L, Ruuskanen O, Allander T, Söderlund-Venermo M. 2012. Human bocavirus—the first 5 years. *Rev Med Virol* 22:46–64. <https://doi.org/10.1002/rmv.720>.
 19. Brodzinski H, Ruddy RM. 2009. Review of new and newly discovered respiratory tract viruses in children. *Pediatr Emerg Care* 25:352–360. <https://doi.org/10.1097/PEC.0b013e3181a3497e>.
 20. Martin ET, Kuypers J, McRoberts JP, Englund JA, Zerr DM. 2015. Human bocavirus-1 primary infection and shedding in infants. *J Infect Dis* 212:516–524. <https://doi.org/10.1093/infdis/jiv044>.
 21. Qiu J, Söderlund-Venermo M, Young NS. 2017. Human parvoviruses. *Clin Microbiol Rev*, in press.
 22. Huang Q, Deng X, Yan Z, Cheng F, Luo Y, Shen W, Lei-Butters DC, Chen AY, Li Y, Tang L, Söderlund-Venermo M, Engelhardt JF, Qiu J. 2012. Establishment of a reverse genetics system for studying human bocavirus in human airway epithelia. *PLoS Pathog* 8:e1002899. <https://doi.org/10.1371/journal.ppat.1002899>.
 23. Deng X, Yan Z, Luo Y, Xu J, Cheng Y, Li Y, Engelhardt J, Qiu J. 2013. In vitro modeling of human bocavirus 1 infection of polarized primary human airway epithelia. *J Virol* 87:4097–4102. <https://doi.org/10.1128/JVI.03132-12>.
 24. Deng X, Li Y, Qiu J. 2014. Human bocavirus 1 infects commercially available primary human airway epithelium cultures productively. *J Virol Methods* 195:112–119. <https://doi.org/10.1016/j.jviromet.2013.10.012>.
 25. Shen W, Deng X, Zou W, Cheng F, Engelhardt JF, Yan Z, Qiu J. 2015. Identification and functional analysis of novel nonstructural proteins of human bocavirus 1. *J Virol* 89:10097–10109. <https://doi.org/10.1128/JVI.01374-15>.
 26. Tewary SK, Zhao H, Shen W, Qiu J, Tang L. 2013. Structure of the NS1 protein N-terminal origin-recognition/nickase domain from the emerging human bocavirus. *J Virol* 87:11487–11494. <https://doi.org/10.1128/JVI.01770-13>.
 27. Chen AY, Cheng F, Lou S, Luo Y, Liu Z, Delwart E, Pintel D, Qiu J. 2010. Characterization of the gene expression profile of human bocavirus. *Virology* 403:145–154. <https://doi.org/10.1016/j.virol.2010.04.014>.
 28. Schildgen O, Qiu J, Soderlund-Venermo M. 2012. Genomic features of the human bocaviruses. *Future Virol* 7:31–39. <https://doi.org/10.2217/fvl.11.136>.
 29. Lederman M, Patton JT, Stout ER, Bates RC. 1984. Virally coded noncapsid protein associated with bovine parvovirus infection. *J Virol* 49:315–318.
 30. Sun Y, Chen AY, Cheng F, Guan W, Johnson FB, Qiu J. 2009. Molecular characterization of infectious clones of the minute virus of canines reveals unique features of bocaviruses. *J Virol* 83:3956–3967. <https://doi.org/10.1128/JVI.02569-08>.
 31. Sukhu L, Fasina O, Burger L, Rai A, Qiu J, Pintel DJ. 2013. Characterization of the nonstructural proteins of the bocavirus minute virus of canines. *J Virol* 87:1098–1104. <https://doi.org/10.1128/JVI.02627-12>.
 32. Fasina OO, Dong Y, Pintel DJ. 2015. NP1 protein of the bocavirus minute virus of canines controls access to the viral capsid genes via its role in RNA processing. *J Virol* 90:1718–1728. <https://doi.org/10.1128/JVI.02618-15>.
 33. Zou W, Cheng F, Shen W, Engelhardt JF, Yan Z, Qiu J. 2016. Nonstructural protein NP1 of human bocavirus 1 plays a critical role in the expression of viral capsid proteins. *J Virol* 90:4658–4669. <https://doi.org/10.1128/JVI.02964-15>.
 34. Mihaylov IS, Cotmore SF, Tattersall P. 2014. Complementation for an essential ancillary non-structural protein function across parvovirus genera. *Virology* 468–470:226–237. <https://doi.org/10.1016/j.virol.2014.07.043>.
 35. Deng X, Yan Z, Cheng F, Engelhardt JF, Qiu J. 2016. Replication of an autonomous human parvovirus in non-dividing human airway epithelium is facilitated through the DNA damage and repair pathways. *PLoS Pathog* 12:e1005399. <https://doi.org/10.1371/journal.ppat.1005399>.
 36. Bashir T, Horlein R, Rommelaere J, Willwand K. 2000. Cyclin A activates the DNA polymerase delta-dependent elongation machinery in vitro: a parvovirus DNA replication model. *Proc Natl Acad Sci U S A* 97:5522–5527. <https://doi.org/10.1073/pnas.090485297>.
 37. Bashir T, Rommelaere J, Cziepluch C. 2001. In vivo accumulation of cyclin A and cellular replication factors in autonomous parvovirus minute virus of mice-associated replication bodies. *J Virol* 75:4394–4398. <https://doi.org/10.1128/JVI.75.9.4394-4398.2001>.
 38. Cotmore SF, Tattersall P. 1987. The autonomously replicating parvoviruses of vertebrates. *Adv Virus Res* 33:91–174. [https://doi.org/10.1016/S0065-3527\(08\)60317-6](https://doi.org/10.1016/S0065-3527(08)60317-6).
 39. Luo Y, Deng X, Cheng F, Li Y, Qiu J. 2013. SMC1-mediated intra-S phase arrest facilitates bocavirus DNA replication. *J Virol* 87:4017–4032. <https://doi.org/10.1128/JVI.03396-12>.
 40. Luo Y, Kleiboeker S, Deng X, Qiu J. 2013. Human parvovirus B19 infection causes cell cycle arrest of human erythroid progenitors at late S phase that favors viral DNA replication. *J Virol* 87:12766–12775. <https://doi.org/10.1128/JVI.02333-13>.
 41. Berns KI, Parrish CR. 2015. Parvoviridae, p 1768–1791. *In* Knipe DM, Howley PM, Cohen JL, Griffin DE, Lamb RA, Martin MA, Racaniello VR, Roizman B (ed), *Fields virology*, 6th ed. Lippincott Williams & Wilkins, Philadelphia, PA.
 42. Kailasan S, Agbandje-McKenna M, Parrish CR. 2015. Parvovirus family conundrum: what makes a killer? *Annu Rev Virol* 2:425–450. <https://doi.org/10.1146/annurev-virology-100114-055150>.
 43. Yan Z, Keiser NW, Song Y, Deng X, Cheng F, Qiu J, Engelhardt JF. 2013. A novel chimeric adenoassociated virus 2/human bocavirus 1 parvovirus vector efficiently transduces human airway epithelia. *Mol Ther* 21:2181–2194. <https://doi.org/10.1038/mt.2013.92>.
 44. Block WD, Yu Y, Lees-Miller SP. 2004. Phosphatidylinositol 3-kinase-like serine/threonine protein kinases (PIKKs) are required for DNA damage-induced phosphorylation of the 32 kDa subunit of replication protein A at threonine 21. *Nucleic Acids Res* 32:997–1005. <https://doi.org/10.1093/nar/gkh265>.
 45. Mah LJ, El-Osta A, Karagiannis TC. 2010. gammaH2AX: a sensitive mo-

- lecular marker of DNA damage and repair. *Leukemia* 24:679–686. <https://doi.org/10.1038/leu.2010.6>.
46. Bakkenist CJ, Kastan MB. 2003. DNA damage activates ATM through intermolecular autophosphorylation and dimer dissociation. *Nature* 421: 499–506. <https://doi.org/10.1038/nature01368>.
 47. Liu S, Shiotani B, Lahiri M, Marechal A, Tse A, Leung CC, Glover JN, Yang XH, Zou L. 2011. ATR autophosphorylation as a molecular switch for checkpoint activation. *Mol Cell* 43:192–202. <https://doi.org/10.1016/j.molcel.2011.06.019>.
 48. Yajima H, Lee KJ, Zhang S, Kobayashi J, Chen BP. 2009. DNA double-strand break formation upon UV-induced replication stress activates ATM and DNA-PKcs kinases. *J Mol Biol* 385:800–810. <https://doi.org/10.1016/j.jmb.2008.11.036>.
 49. Soubeyrand S, Pope L, Pakuts B, Hache RJ. 2003. Threonines 2638/2647 in DNA-PK are essential for cellular resistance to ionizing radiation. *Cancer Res* 63:1198–1201.
 50. Luo Y, Chen AY, Qiu J. 2011. Bocavirus infection induces a DNA damage response that facilitates viral DNA replication and mediates cell death. *J Virol* 85:133–145. <https://doi.org/10.1128/JVI.01534-10>.
 51. Olive PL, Banath JP. 2006. The Comet assay: a method to measure DNA damage in individual cells. *Nat Protoc* 1:23–29. <https://doi.org/10.1038/nprot.2006.5>.
 52. Christensen J, Tattersall P. 2002. Parvovirus initiator protein NS1 and RPA coordinate replication fork progression in a reconstituted DNA replication system. *J Virol* 76:6518–6531. <https://doi.org/10.1128/JVI.76.13.6518-6531.2002>.
 53. Nash K, Chen W, Muzyczka N. 2008. Complete in vitro reconstitution of adeno-associated virus DNA replication requires the minichromosome maintenance complex proteins. *J Virol* 82:1458–1464. <https://doi.org/10.1128/JVI.01968-07>.
 54. Soderberg O, Gullberg M, Jarvius M, Ridderstrale K, Leuchowius KJ, Jarvius J, Wester K, Hydbring P, Bahram F, Larsson LG, Landegren U. 2006. Direct observation of individual endogenous protein complexes in situ by proximity ligation. *Nat Methods* 3:995–1000. <https://doi.org/10.1038/nmeth947>.
 55. Yang W. 2014. An overview of Y-family DNA polymerases and a case study of human DNA polymerase eta. *Biochemistry* 53:2793–2803. <https://doi.org/10.1021/bi500019s>.
 56. Cotmore SF, Tattersall P. 2014. Parvoviruses: small does not mean simple. *Annu Rev Virol* 1:517–537. <https://doi.org/10.1146/annurev-virology-031413-085444>.
 57. Chen AY, Qiu J. 2010. Parvovirus infection-induced cell death and cell cycle arrest. *Future Virol* 5:731–741. <https://doi.org/10.2217/fvl.10.56>.
 58. Cotmore SF, Tattersall P. 2013. Parvovirus diversity and DNA damage responses. *Cold Spring Harb Perspect Biol* 5:a012989. <https://doi.org/10.1101/cshperspect.a012989>.
 59. Luo Y, Qiu J. 2013. Parvovirus infection induced DNA damage response. *Future Virol* 8:245–257. <https://doi.org/10.2217/fvl.13.5>.
 60. Ciccia A, Elledge SJ. 2010. The DNA damage response: making it safe to play with knives. *Mol Cell* 40:179–204. <https://doi.org/10.1016/j.molcel.2010.09.019>.
 61. Luftig MA. 2014. Viruses and the DNA damage response: activation and antagonism. *Annu Rev Virol* 1:605–625. <https://doi.org/10.1146/annurev-virology-031413-085548>.
 62. Liang X, Pickering MT, Cho NH, Chang H, Volkert MR, Kowalik TF, Jung JU. 2006. Dereglulation of DNA damage signal transduction by herpesvirus latency-associated M2. *J Virol* 80:5862–5874. <https://doi.org/10.1128/JVI.02732-05>.
 63. Belgnaoui SM, Fryrear KA, Nyalwidhe JO, Guo X, Semmes OJ. 2010. The viral oncoprotein Tax sequesters DNA damage response factors by tethering MDC1 to chromatin. *J Biol Chem* 285:32897–32905. <https://doi.org/10.1074/jbc.M110.146373>.
 64. Durkin SS, Guo X, Fryrear KA, Mihaylova VT, Gupta SK, Belgnaoui SM, Haoudi A, Kupfer GM, Semmes OJ. 2008. HTLV-1 Tax oncoprotein subverts the cellular DNA damage response via binding to DNA-dependent protein kinase. *J Biol Chem* 283:36311–36320. <https://doi.org/10.1074/jbc.M804931200>.
 65. Rogakou EP, Boon C, Redon C, Bonner WM. 1999. Megabase chromatin domains involved in DNA double-strand breaks in vivo. *J Cell Biol* 146:905–916. <https://doi.org/10.1083/jcb.146.5.905>.
 66. Stucki M, Clapperton JA, Mohammad D, Yaffe MB, Smerdon SJ, Jackson SP. 2005. MDC1 directly binds phosphorylated histone H2AX to regulate cellular responses to DNA double-strand breaks. *Cell* 123:1213–1226. <https://doi.org/10.1016/j.cell.2005.09.038>.
 67. Golding SE, Rosenberg E, Valerie N, Hussaini I, Frigerio M, Cockcroft XF, Chong WY, Hummersone M, Rigoreau L, Menear KA, O'Connor MJ, Povirk LF, van Meter T, Valerie K. 2009. Improved ATM kinase inhibitor KU-60019 radiosensitizes glioma cells, compromises insulin, AKT and ERK prosurvival signaling, and inhibits migration and invasion. *Mol Cancer Ther* 8:2894–2902. <https://doi.org/10.1158/1535-7163.MCT-09-0519>.
 68. Charrier JD, Durrant SJ, Golec JM, Kay DP, Knegtel RM, MacCormick S, Mortimore M, O'Donnell ME, Pinder JL, Reaper PM, Rutherford AP, Wang PS, Young SC, Pollard JR. 2011. Discovery of potent and selective inhibitors of ataxia telangiectasia mutated and Rad3 related (ATR) protein kinase as potential anticancer agents. *J Med Chem* 54:2320–2330. <https://doi.org/10.1021/jm101488z>.
 69. Arris CE, Boyle FT, Calvert AH, Curtin NJ, Endicott JA, Garman EF, Gibson AE, Golding BT, Grant S, Griffin RJ, Jewsbury P, Johnson LN, Lawrie AM, Newell DR, Noble ME, Sausville EA, Schultz R, Yu W. 2000. Identification of novel purine and pyrimidine cyclin-dependent kinase inhibitors with distinct molecular interactions and tumor cell growth inhibition profiles. *J Med Chem* 43:2797–2804. <https://doi.org/10.1021/jm990628o>.
 70. Chen AY, Kleiboeker S, Qiu J. 2011. Productive parvovirus B19 infection of primary human erythroid progenitor cells at hypoxia is regulated by STAT5A and MEK signaling but not HIF alpha. *PLoS Pathog* 7:e1002088. <https://doi.org/10.1371/journal.ppat.1002088>.
 71. Kerr JR. 2016. The role of parvovirus B19 in the pathogenesis of autoimmunity and autoimmune disease. *J Clin Pathol* 69:279–291. <https://doi.org/10.1136/jclinpath-2015-203455>.
 72. Chen AY, Guan W, Lou S, Liu Z, Kleiboeker S, Qiu J. 2010. Role of erythropoietin receptor signaling in parvovirus B19 replication in human erythroid progenitor cells. *J Virol* 84:12385–12396. <https://doi.org/10.1128/JVI.01229-10>.
 73. Luo Y, Lou S, Deng X, Liu Z, Li Y, Kleiboeker S, Qiu J. 2011. Parvovirus B19 infection of human primary erythroid progenitor cells triggers ATR-Chk1 signaling, which promotes B19 virus replication. *J Virol* 85:8046–8055. <https://doi.org/10.1128/JVI.00831-11>.